Prompt Atmospheric neutrino fluxes: The role of parton distribution functions and constraints on intrinsic charm

1. Basics: Calculation of atmospheric lepton fluxes
2. QCD predictions and experimental data on charmed hadron production
3. Contribution of intrinsic charm

based on work by Garzelli, Moch, Ostapchenko, Sigl and PROSA collaboration

PROJEKTTRÄGER FÜR DAS
Bundesministerium
für Bildung
und Forschung

CLUSTER OF EXCELLENCE
QUANTUM UNIVERSE

Universität Hamburg
DER FORSCHUNG | DER LEHRE | DER BILDUNG

Günter Sigl
II. Institut theoretische Physik, Universität Hamburg

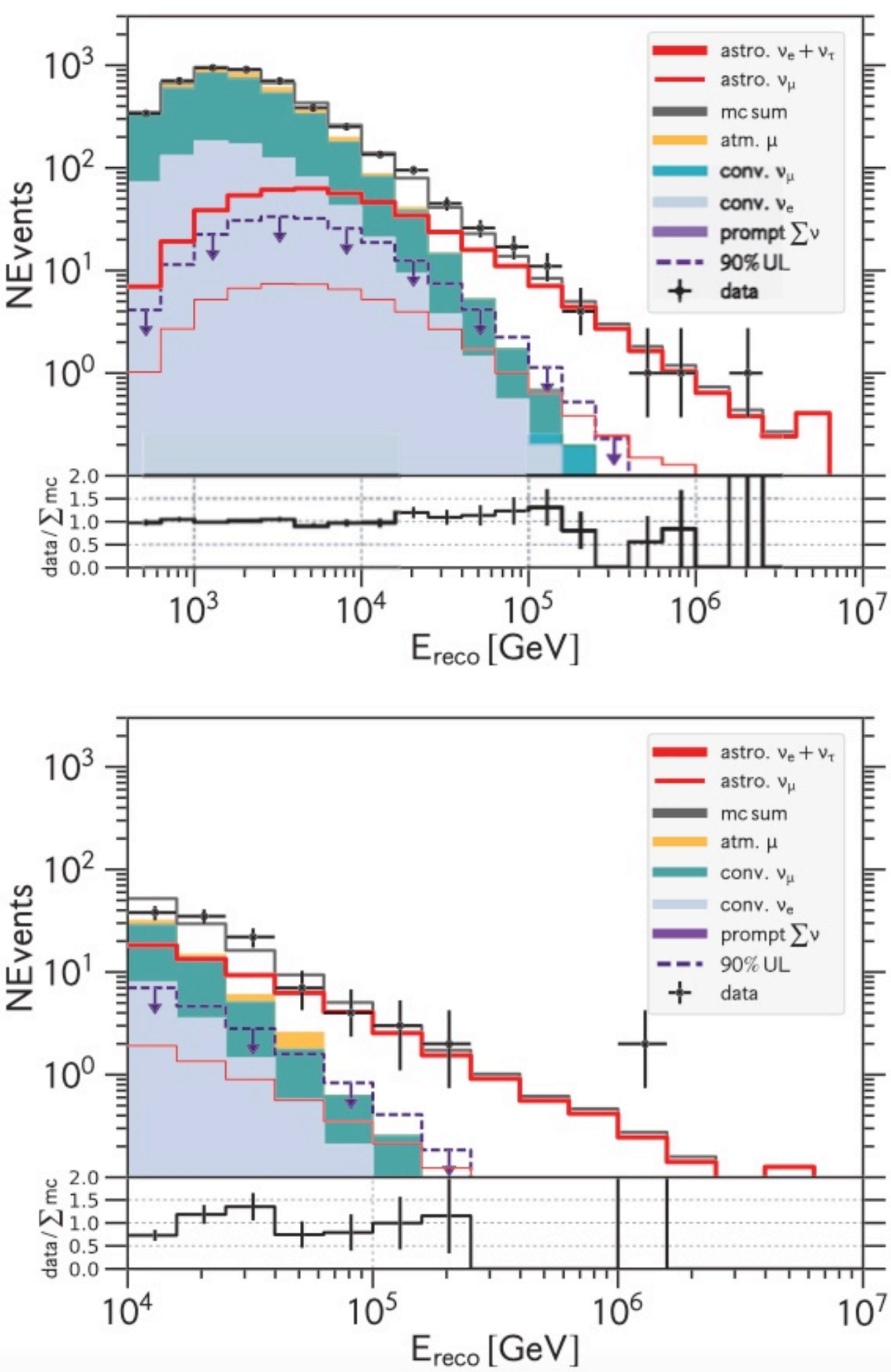

Components of the Diffuse Spectrum

astrophysical neutrinos have a harder spectrum than atmospheric neutrinos which have a spectrum steeper by one power of energy than cosmic ray spectrum due to energy-dependent decay probability of pions, thus $\sim E^{-3.7}$

flavour ratio $(\nu_e + \bar{\nu}_e)/(\nu_\mu + \bar{\nu}_\mu) \sim 1$ for astrophysical neutrinos, but $(\nu_e + \bar{\nu}_e)/(\nu_\mu + \bar{\nu}_\mu) \sim 0.3(10\,\mathrm{GeV}/E_\nu)$ for $E_\nu \gtrsim \mathrm{GeV}$ due to energy-dependent decay probability of muons; flavour ratio saturates at few percent level above ~ 100 GeV due to kaon production.

Aartsen et al [IceCube collaboration], PRL 125 (2020) 121104 [arXiv:1807.11492]

Introduction/Reminder on atmospheric neutrinos

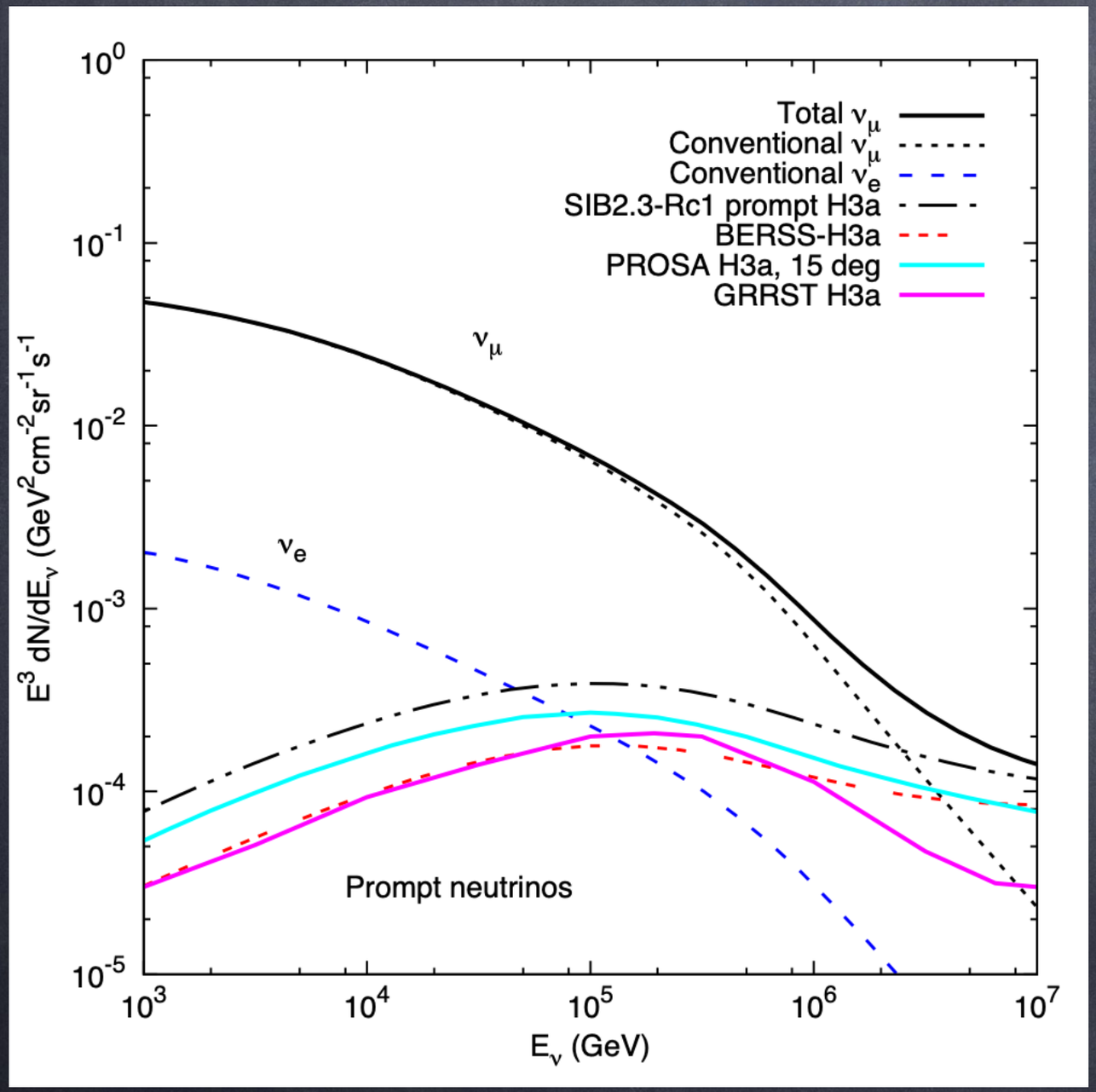

$$p + {}^{A}_{Z} \rightarrow {}^{A'}_{Z'} + \pi^{\pm}/K^{\pm} + \cdots$$

$$\pi^{\pm}/K^{\pm} \rightarrow \mu^{+}(\mu^{-}) + \nu_\mu(\bar{\nu}_\mu)$$

$$\mu^{+}(\mu^{-}) \rightarrow e^{+}(e^{-}) + \nu_e(\bar{\nu}_e) + \bar{\nu}_\mu(\nu_\mu)$$

Conventional neutrino fluxes from decays of light mesons and other light hadrons are suppressed by one power in energy compared to the primary nucleon flux at high energies due to the charged pion decay probability $\sim (20\,\mathrm{GeV}/E_\pi)$

Prompt neutrino fluxes from decays of heavy mesons and other hadrons follow roughly the primary nucleon flux at high energies

Gaisser, arXiv:1910.08851

Atmospheric neutrino fluxes

after M.V. Garzelli

CR + *Air* interactions:
- AA' interaction approximated as $A\ NA'$ interactions (superposition);
- NA' approximated as $A'\ NN$ interactions: up to which extent is this valid ?

* conventional neutrino flux:

$$NN \rightarrow u,d,s,\bar{u},\bar{d},\bar{s} + X \rightarrow \pi^{\pm}, K^{\pm} + X' \rightarrow \nu_\ell(\bar{\nu}_\ell) + \ell^{\pm} + X',$$
$$NN \rightarrow u,d,s,\bar{u},\bar{d},\bar{s} + X \rightarrow K^0_S,\ K^0_L + X \rightarrow \pi^{\pm} + \ell^{\mp} + \nu_{\overset{(-)}{\ell}} + X$$
$$NN \rightarrow u,d,s,\bar{u},\bar{d},\bar{s} + X \rightarrow \textit{light hadron} + X' \rightarrow \nu(\bar{\nu}) + X''$$

* prompt neutrino flux:

$$NN \rightarrow c,b,\bar{c},\bar{b} + X \rightarrow \textit{heavy-hadron} + X' \rightarrow \nu(\bar{\nu}) + X'' + X'$$

where the decay to neutrino occurs through semileptonic and leptonic decays:

$D^+ \rightarrow e^+\nu_e X$, $D^+ \rightarrow \mu^+\nu_\mu X$,
$D_s^{\pm} \rightarrow \nu_\tau(\bar{\nu}_\tau) + \tau^{\pm}$, with further decay $\tau^{\pm} \rightarrow \nu_\tau(\bar{\nu}_\tau) + X$

proper decay lenghts: $c\tau_{0,\pi^{\pm}} = 780$ cm, $c\tau_{0,K^{\pm}} = 371$ cm, $c\tau_{0,D^{\pm}} = 0.031$ cm

Critical energy $\epsilon_h = m_h c^2 h_0 \,/\, (c\,\tau_{0,h}\cos(\theta))$, above which hadron **decay** probability is suppressed with respect to its **interaction** probability:

$\epsilon_\pi^{\pm} < \epsilon_K^{\pm} << \epsilon_D \Rightarrow$ conventional flux is suppressed with respect to prompt one, for energies high enough, due to finite atmosphere height h_0.

Calculation of Atmospheric Lepton Fluxes

$$\frac{d\phi_j}{dX} = -\frac{\phi_j}{\lambda_{j,int}} - \frac{\phi_j}{\lambda_{j,dec}} + \sum_{k\neq j} S_{\rm prod}(k \to j) + \sum_{k\neq j} S_{\rm decay}(k \to j) + S_{\rm reg}(j \to j)\,.$$

These are known as cascade equations. There is a critical energy above which interactions dominate over decay; for charged pions it is about 20 GeV (-> conventional neutrino flux) for charmed hadrons it is much higher, > 10^7 GeV (-> prompt neutrino flux with harder spectrum)

$$S_{\rm prod}(k \to j) = \int_{E_j}^{\infty} dE_k \frac{\phi_k(E_k, X)}{\lambda_k(E_k)} \frac{1}{\sigma_k} \frac{d\sigma_{k\to j}(E_k, E_j)}{dE_j} \sim \frac{\phi_k(E_j, X)}{\lambda_k(E_j)} Z_{kj}(E_j)\,,$$

$$S_{\rm decay}(j \to l) = \int_{E_l}^{\infty} dE_j \frac{\phi_j(E_j, X)}{\lambda_j(E_j)} \frac{1}{\Gamma_j} \frac{d\Gamma_{j\to l}(E_j, E_l)}{dE_l} \sim \frac{\phi_j(E_l, X)}{\lambda_j(E_l)} Z_{jl}(E_l)\,.$$

where the Z-moments are, e.g. for interactions

$$Z_{kj}^{\rm int}(E_j) = \int_{E_j}^{+\infty} dE'_k \frac{\phi_k(E'_k, 0)}{\phi_k(E_j, 0)} \frac{\lambda_k^{\rm int}(E_j)}{\lambda_k^{\rm int}(E'_k)} \frac{dn(kA \to jX; E'_k, E_j)}{dE_j}\,,$$

Most relevant for us is the all-nucleon flux which depends both on the all-particle flux and the mass composition

From cosmic ray (CR) all particle spectrum to CR all nucleon spectra

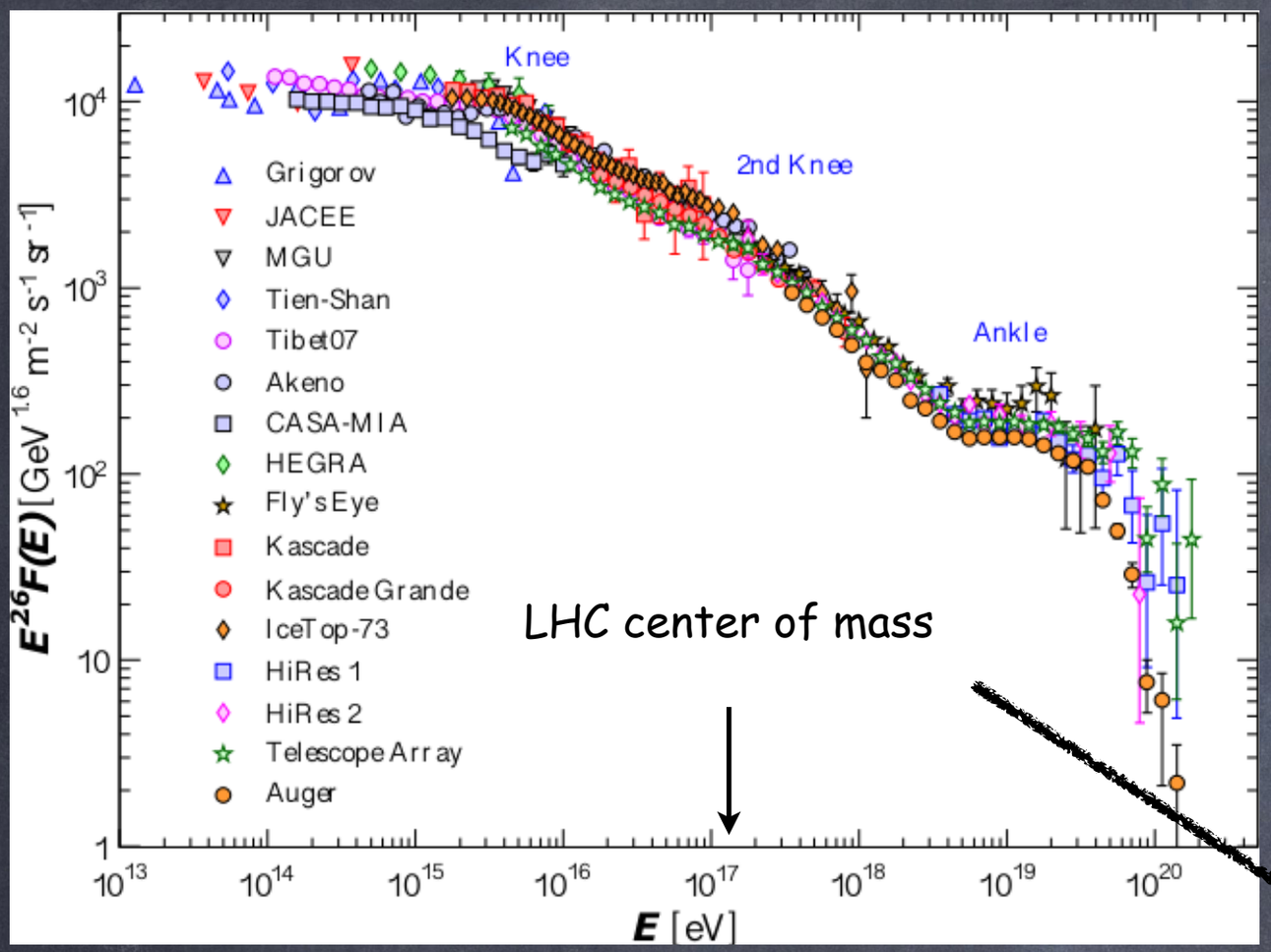

summary of all particle spectrum
from different experiments

under assumption of mass composition ->
flux models used in Garzelli et al., JHEP10 (2015) 115

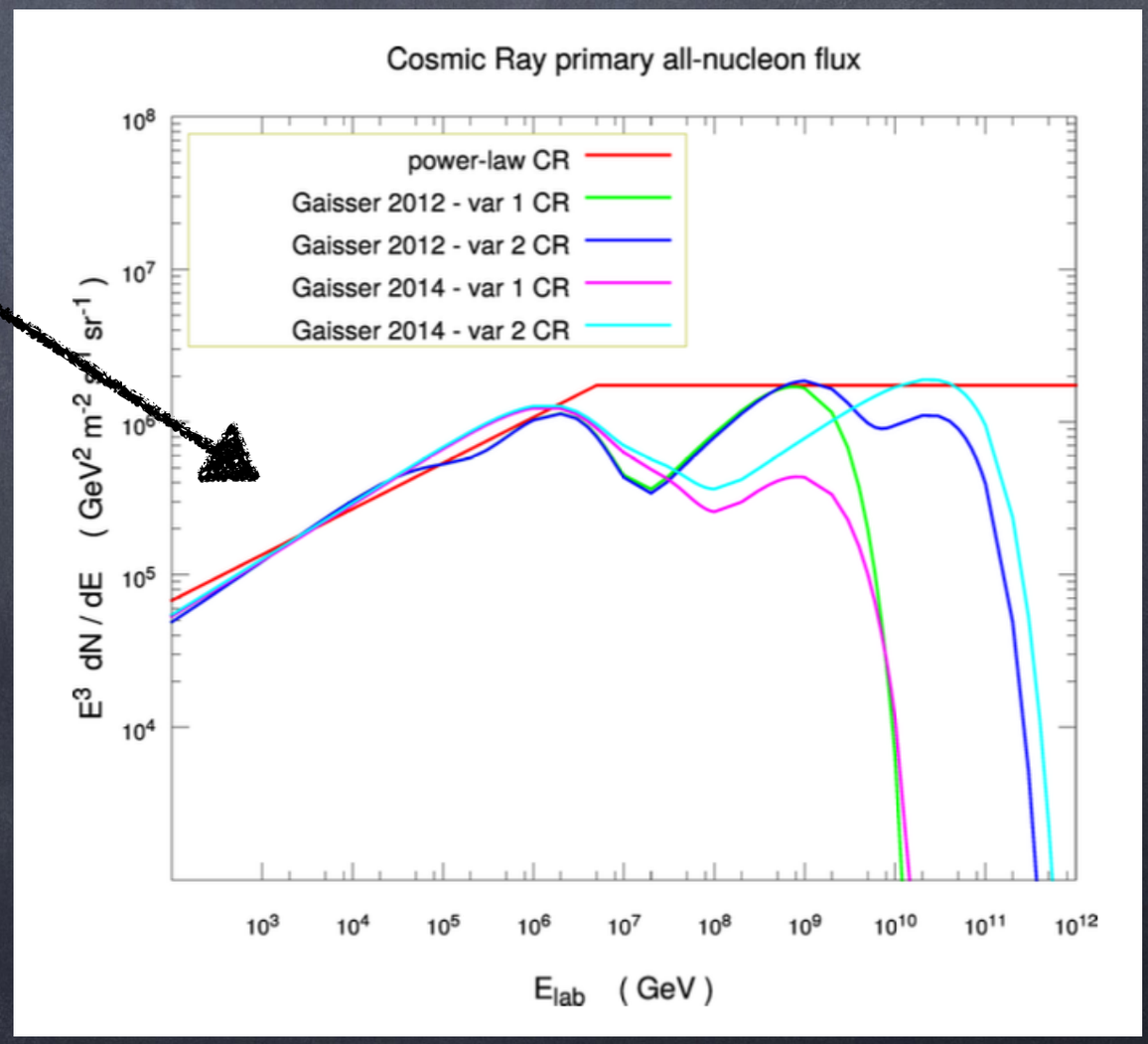

Global Picture on Mass Composition

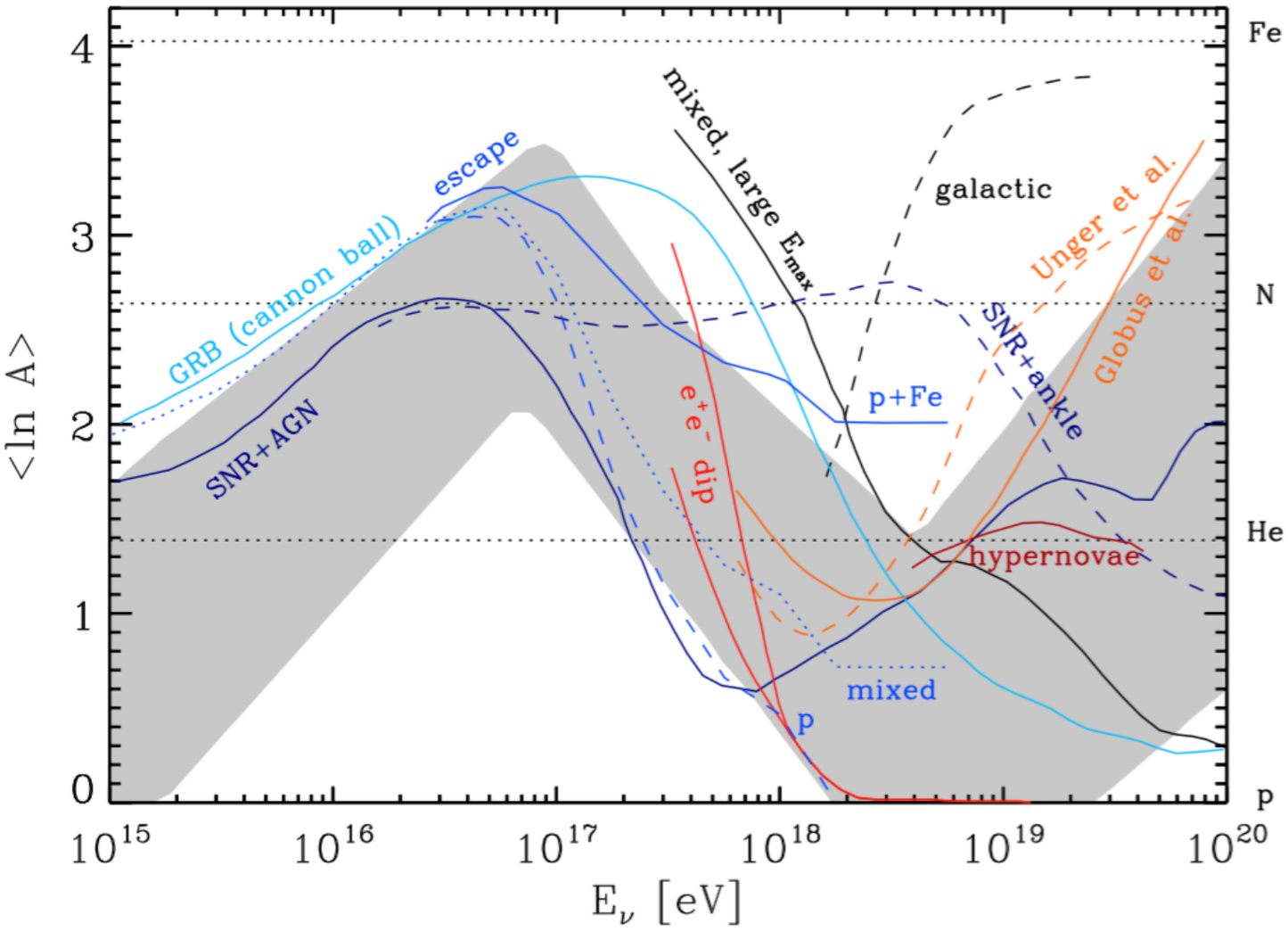

Fig. 5.8 The energy dependence of the average logarithmic mass predicetd by various models, as indicated and explained in more details in the text. The grey band represents the combined uncertainties resulting from systematic experimental errors and hadronic model uncertainties, based on data such as the ones shown in Fig. 5.7. The first minimum in $\langle \ln A \rangle$ at $\simeq 3 \times 10^{15}$ eV corresponds to the CR knee and the first maximum in $\langle \ln A \rangle$ at $\simeq 10^{17}$ eV corresponds to the *second knee*. Both the knee and the second knee could signify a rigidity dependent Peters cycle either due to the maximal rigidity reached at acceleration in supernova remnants or due to a transition to a propagation regime leading to faster CR leakage from the Galaxy. Finally, the second minimum in $\langle \ln A \rangle$ at $\simeq 5 \times 10^{18}$ eV signifies the *ankle*. Compare the CR spectrum shown in Fig. 5.6. Inspired by Ref. [231].

Indications of "Peters cycles" for galactic and extragalactic sources whose maximal energies are proportional to the charge Z and extend up to ~ 10^{17} and 10^{20} eV, respectively

G. Sigl, book "Astroparticle Physics: Theory and Phenomenology", Atlantis Press/Springer 2016

see also K.-H.Kampert and M.Unger, Astropart.Phys. 35 (2012) 660

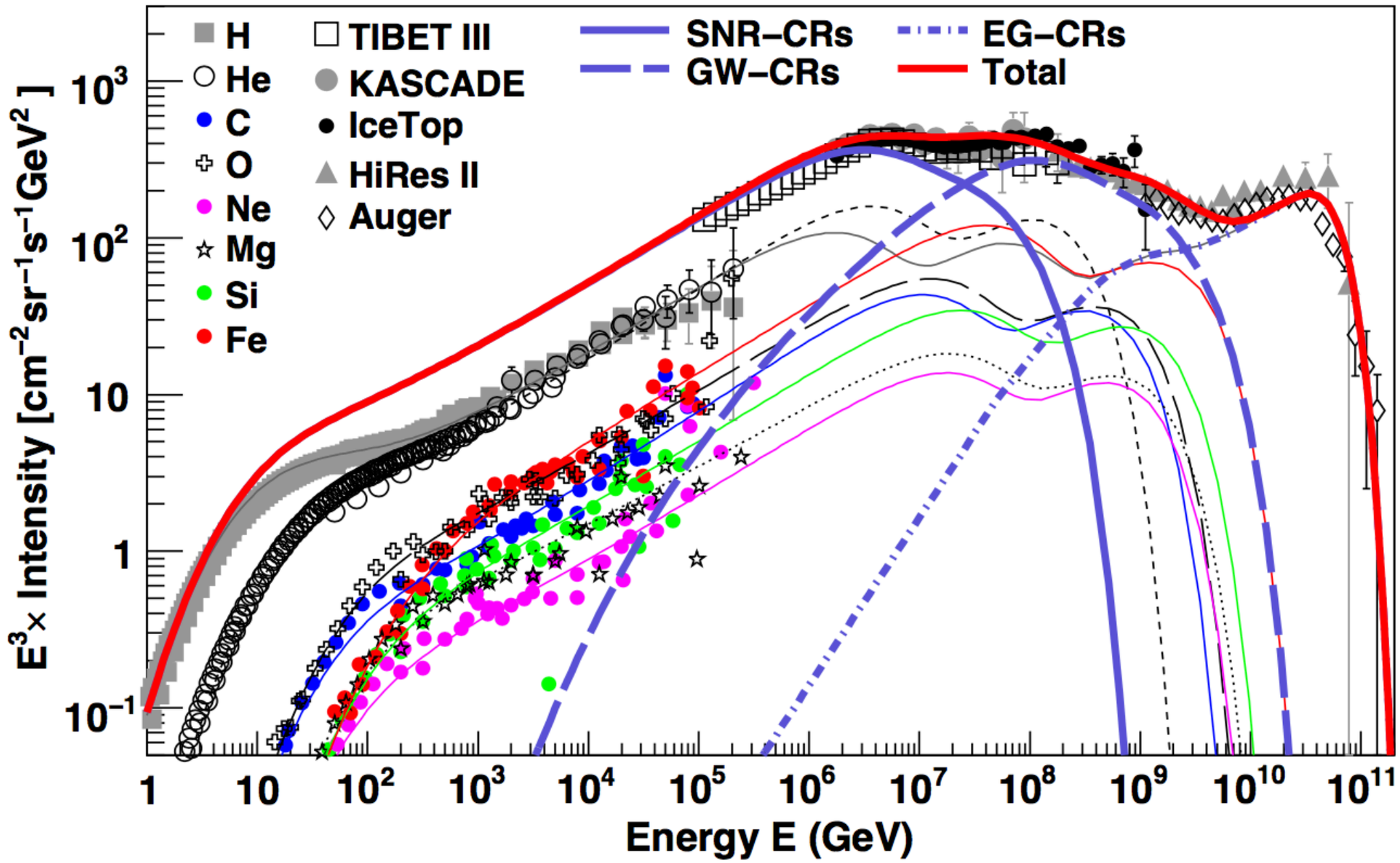

Fig. 5. Model prediction for the all-particle spectrum using the Galactic wind re-acceleration model. The thick solid blue line represents the total SNR-CRs, the thick dashed line represents GW-CRs, the thick dotted-dashed line represents EG-CRs, and the thick solid red line represents the total all-particle spectrum. The thin lines represent total spectra for the individual elements. For the SNR-CRs, an exponential energy cut-off for protons at $E_c = 3 \times 10^6$ GeV is assumed. See text for the other model parameters. Data are the same as in Figure 2.

S. Thoudam et al., A&A 595, A33 (2016) [arXiv:1605.03111]

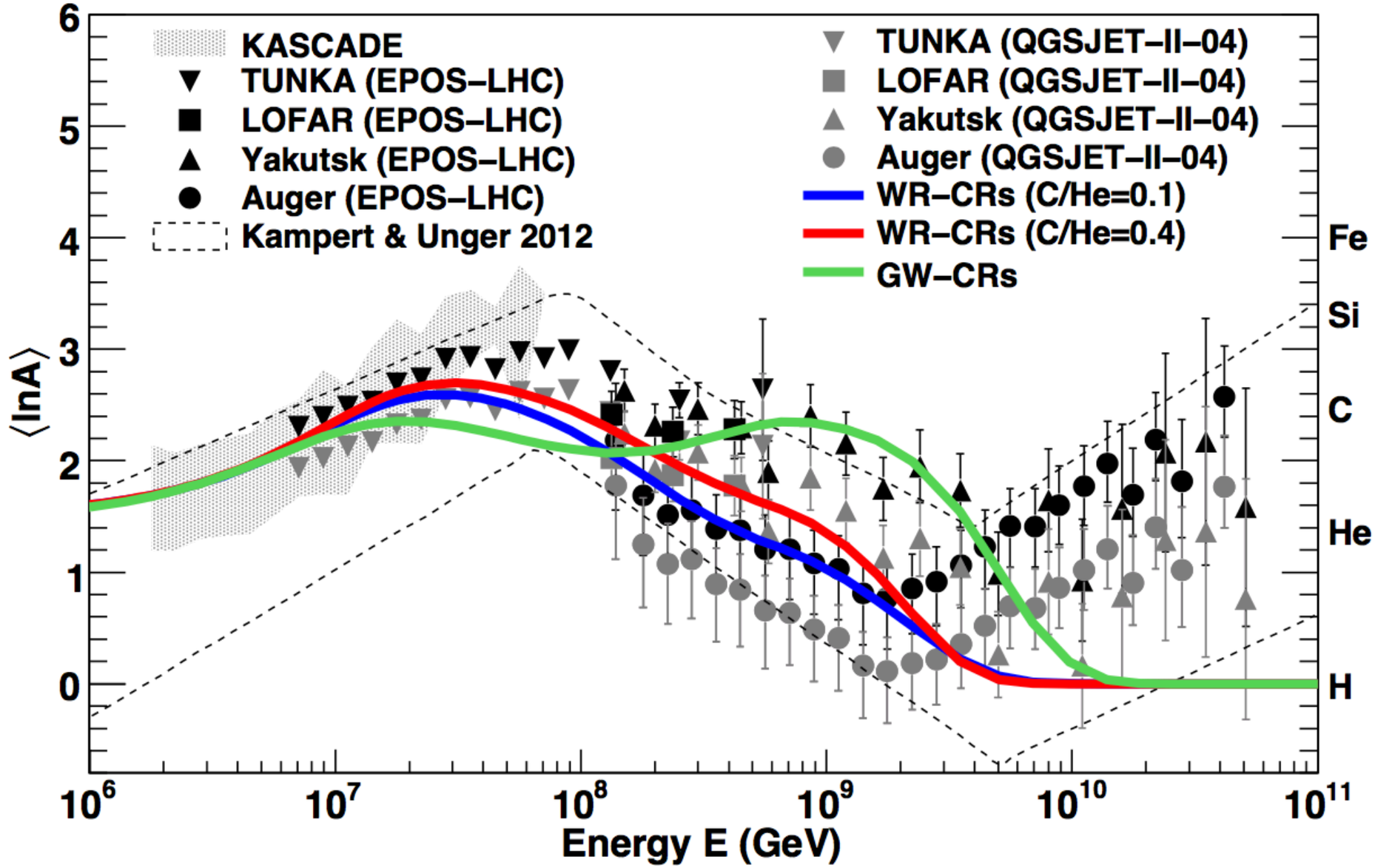

Fig. 8. Mean logarithmic mass, $\langle \ln A \rangle$, of cosmic rays predicted using the three different models of the additional Galactic component: WR-CRs (C/He = 0.1), WR-CRs (C/He = 0.4), and GW-CRs. *Data*: KASCADE (Antoni et al. 2005), TUNKA (Berezhnev et al. 2013), LOFAR (Buitink et al. 2016), Yakutsk (Knurenko & Sabourov 2010), the Pierre Auger Observatory (Porcelli et al. 2015), and the different optical measurements compiled in Kampert & Unger (2012). The two sets of data points correspond to two different hadronic interaction models (EPOS-LHC and QGSJET-II-04) used to convert $X_{\max}$ values to $\langle \ln A \rangle$.

S. Thoudam et al., A&A 595, A33 (2016) [arXiv:1605.03111]

QCD Predictions and Experimental Data on charmed hadron production

Charmed hadron production cross sections depend on parton distribution functions (PDF) and fragmentation functions (FF) which in turn depend on μ_f^2 and x and z (longitudinal momentum fractions), respectively.

Dependence on μ_f^2 can be treated perturbatively, whereas x and z dependence contains non-perturbative effects. The theoretical predictions for the partonic cross sections depend on charm quark (pole) mass, factorisation and renormalisation scales (assuming collinear factorisation)

$$\sigma_{pp\to D+X} = \sum_{i,j} \mathrm{PDF}(x_i, \mu_f^2)\, \mathrm{PDF}(x_j, \mu_f^2) \otimes \hat{\sigma}_{ij\to cX}(x_i, x_j, \mu_f, \mu_r, m_c, z) \otimes \mathrm{FF}_{c\to D}(z, \mu_f^2)$$

Idea is to fit the non-perturbative components of PDFs and FFs with as many measurements as possible to minimise uncertainties when extrapolating to energies and phase space inaccessible to direct experiments but relevant for cosmic ray physics.

$$pp \to D^{\pm} + X \text{ at } \sqrt{s} = 13 \text{ TeV},$$

PROSA 2015 PDF, data: LHCb collaboration, JHEP 03 (2016) 159, and erratum 09 (2016) 013

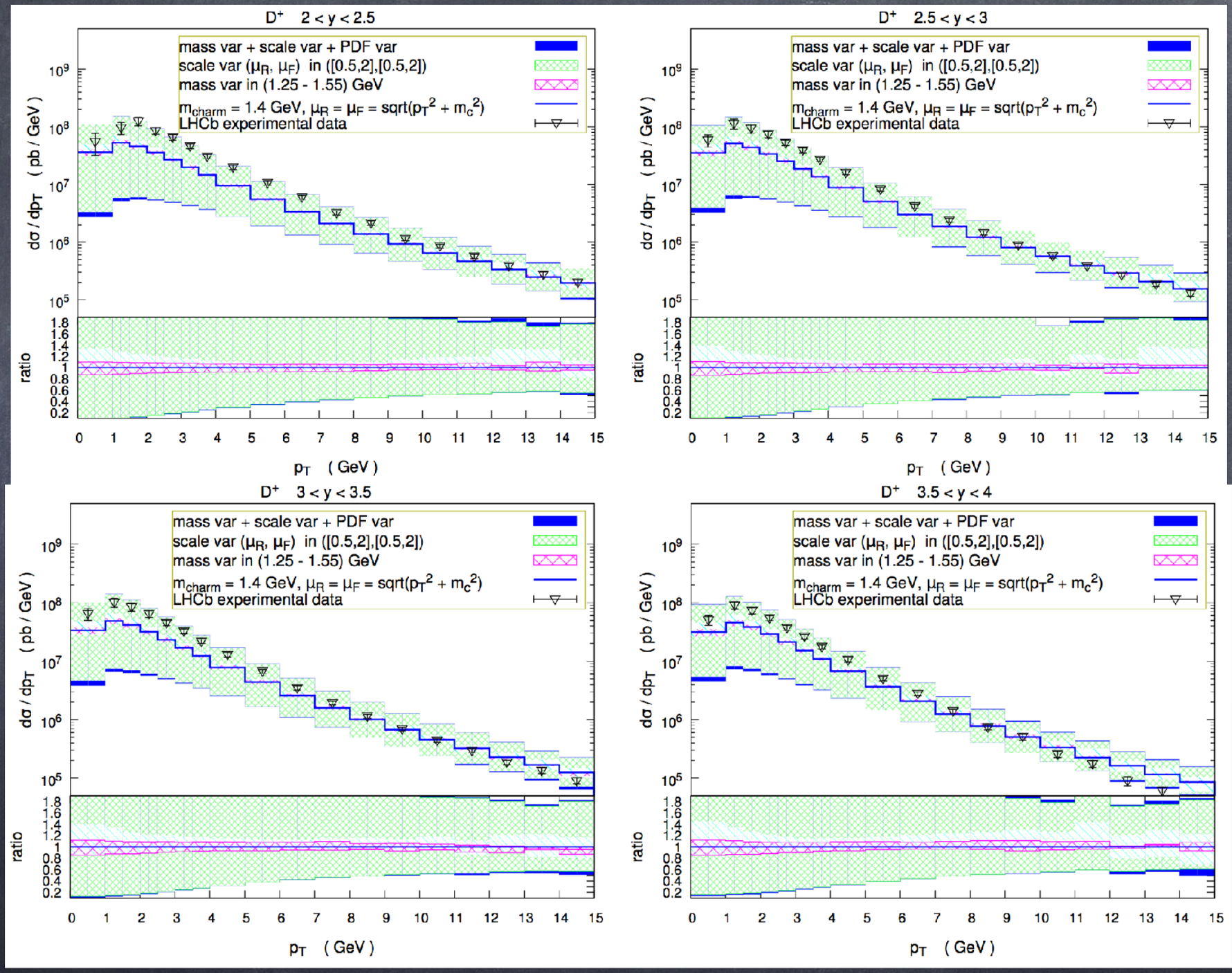

differential cross sections are NLO predictions, only total cross section is known to NNLO

M. Garzelli et al., JHEP 05 (2017) 004 [arXiv:1611.03815]

Comments

theoretical uncertainties larger than experimental uncertainties on D meson production cross section; this can be reduced, however, by taking ratios of suitable quantities (e.g. at different energies or at different rapidities at same energy), as also pointed out by LHCb collaboration.

theoretical cross sections known to NLO for $d\sigma/dp_T$ (not yet NNLO) and to NNLO for total cross section σ

PDFs used in literature:
ABMP16, CT18, JR14, CJ15, HERAPDF, MSHT, …
specifically constrained at low x with LHCb data : PROSA and NNPDF

comparison of parton distribution functions

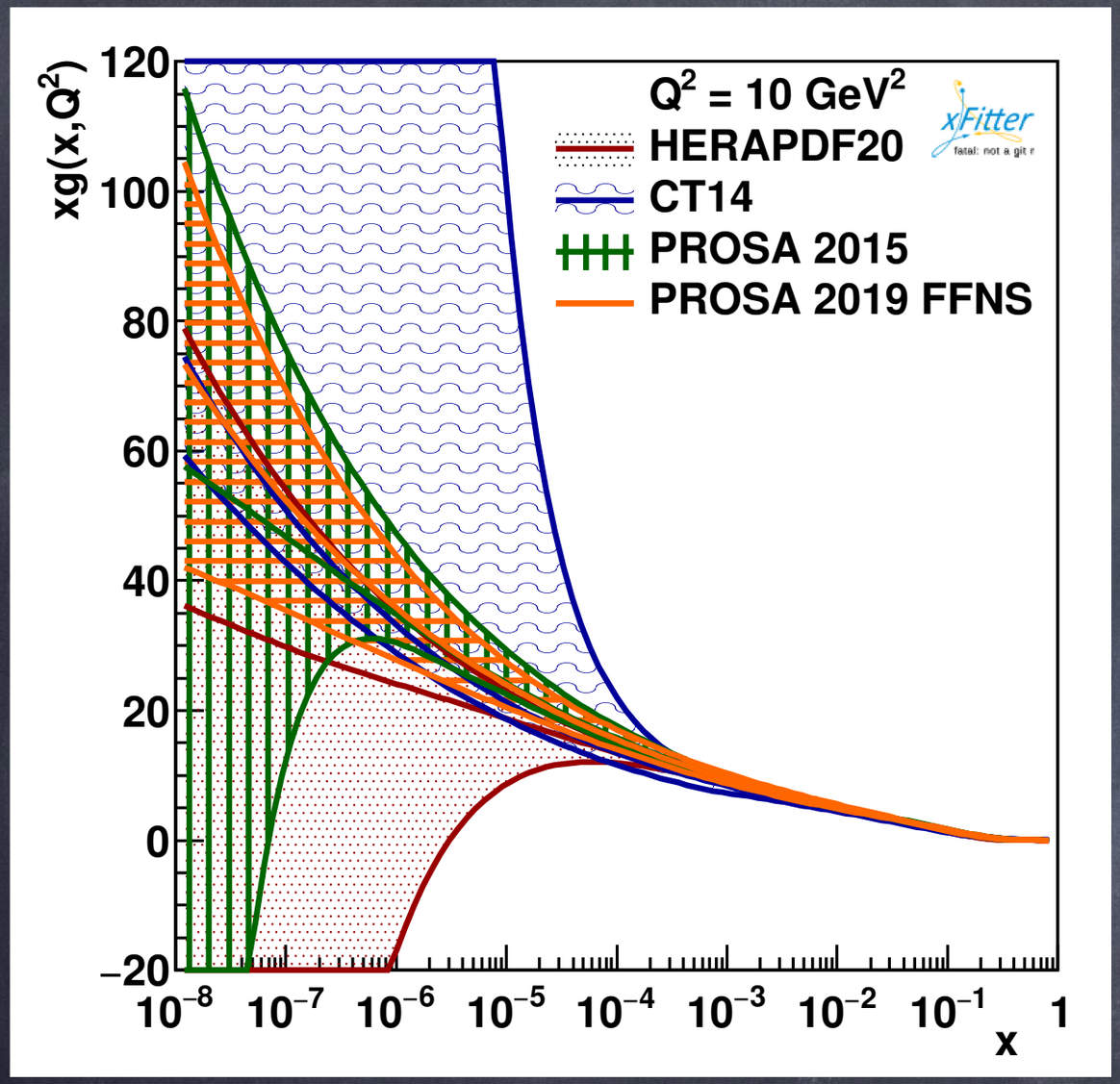

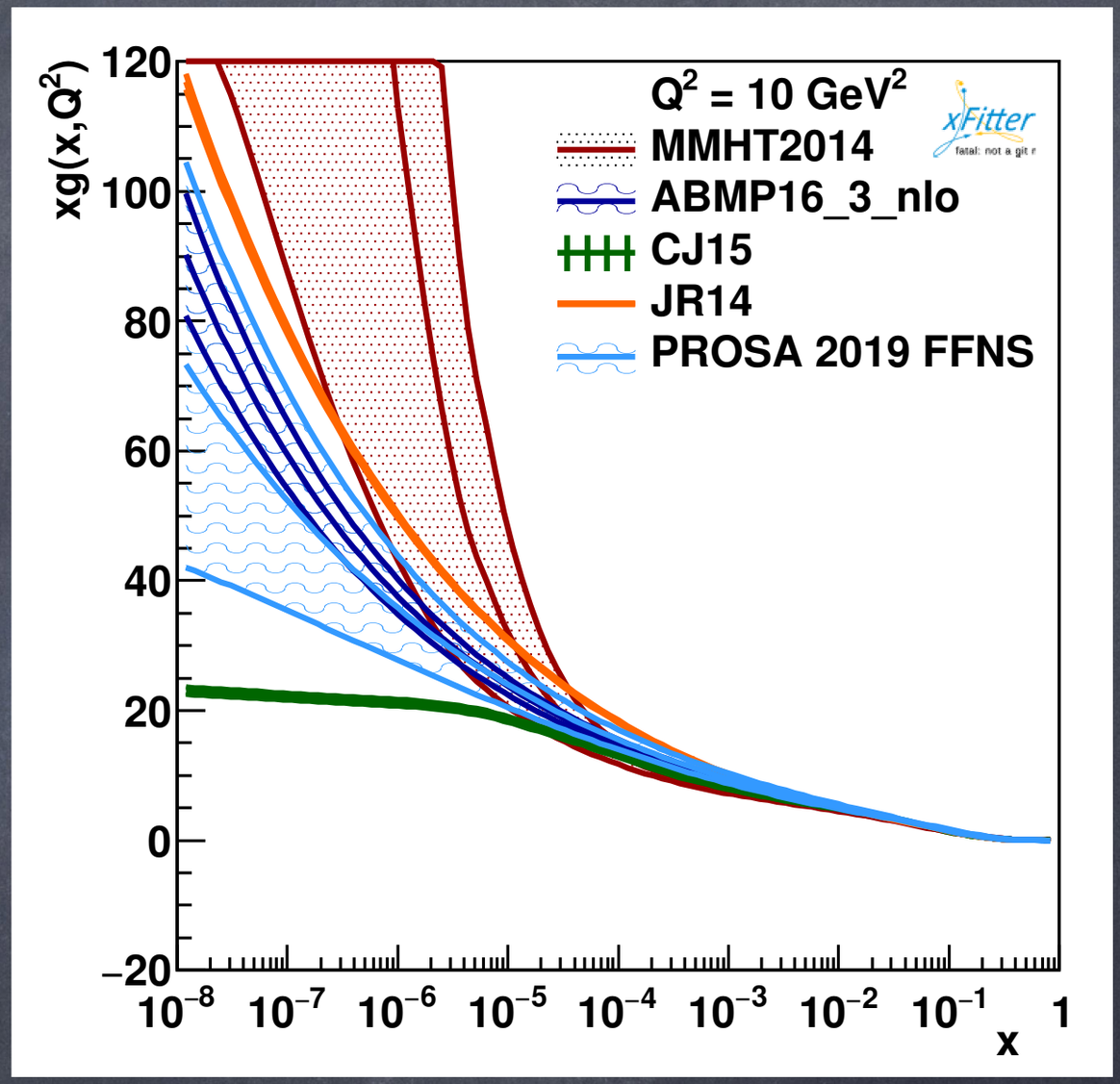

The PROSA2019 gluon distribution compared to PROSA2015, CT14, HERAPDF20 (left panel), and MMHT2014, ABMP16, CJ15, JR14 (right panel)
The PROSA PDF uncertainty at small x is smaller than for other PDFs due to the inclusion of LHCb (and ALICE at large x) heavy-flavor production data

O. Zenaiev et al., JHEP 04 (2020) 118 [arXiv:1911.13184]

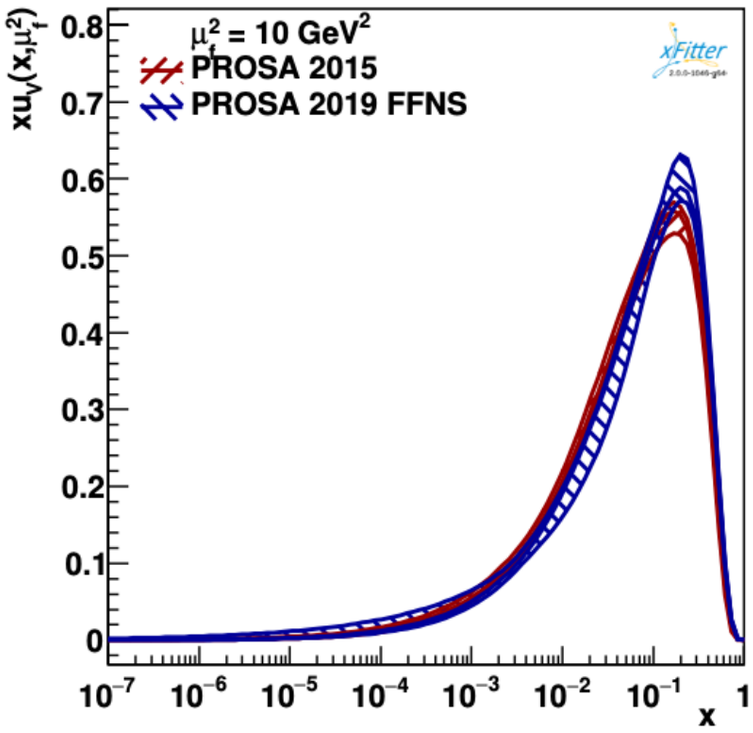

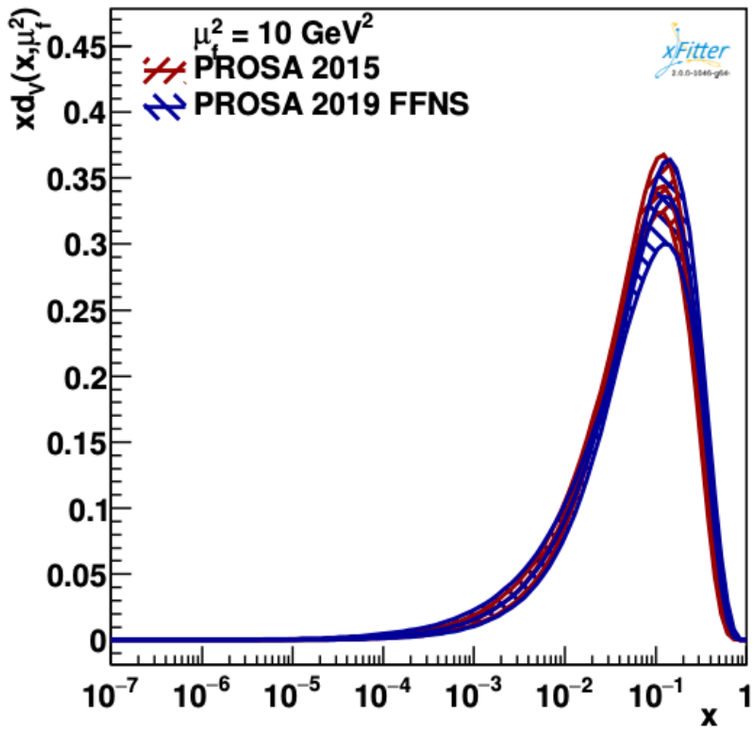

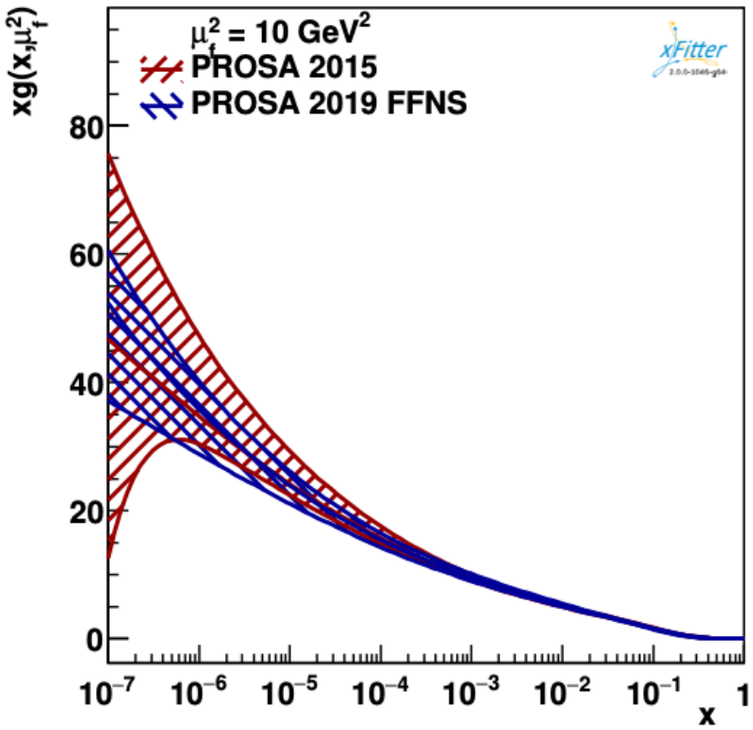

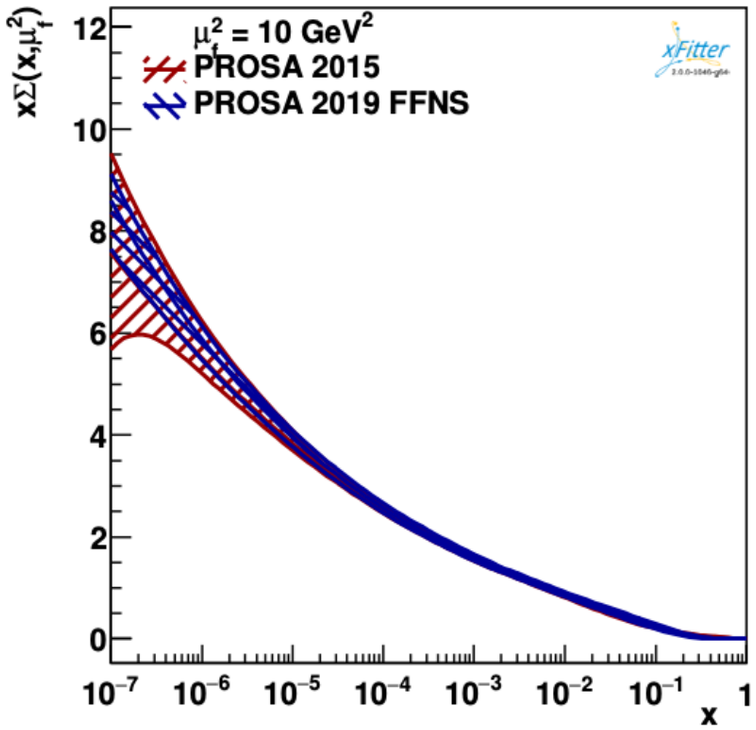

O. Zenaiev et al., JHEP 04 (2020) 118 [arXiv:1911.13184]

Figure 3. The PROSA 2019 PDF in FFNS with their total uncertainties as a function of x shown at the scale $\mu_f^2 = 10\,\mathrm{GeV}^2$, compared with the respective distributions from the PROSA 2015 fit.

u and d quark valence PDFs

right panel: sum over all sea quarks:
LHCb data is relevant for also constraining sea quark PDFs, but they provide a subdominant contribution to prompt neutrino fluxes
PROSA 2019 includes 5, 7, 13 TeV data whereas PROSA 2015 only includes 7 TeV data

Alternative Method for Z-moment computation

For power law CR primary proton spectra $I_p(E_p) \propto E_p^{-\gamma_p}$ one can write the prompt muon neutrino spectrum as

$$I^{(p)}_{\nu_\mu(\text{prompt})}(E_\nu) \simeq \frac{I_p(E_\nu)}{1 - Z^p_{p-\text{air}}(E_\nu, \gamma_p)} \, Z^{\nu_\mu(\text{prompt})}_{p-\text{air}}(E_\nu, \gamma_p) \, .$$

Factorisation of the proton-to-neutrino Z-moment into pQCD dependent proton-to-charm quark moment and fragmentation and decay moments leads to

$$Z^{\nu_\mu(\text{prompt})}_{p-\text{air}}(E_\nu, \gamma_p) \simeq Z^{c}_{p-\text{air}}(E_\nu, \gamma_p) \left[\sum_{c,\bar{c}} \sum_{h_c} Z^{\text{fragm}}_{c\,(\bar{c})\to h_c}(\gamma_p) \, Z^{\text{dec}}_{h_c \to \nu_\mu}(\gamma_p) \right],$$

where

$$Z^{c}_{p-\text{air}}(E, \gamma) \simeq \int dx_c \; x_c^{\gamma-1} \frac{\langle A_{\text{air}} \rangle}{\sigma^{\text{inel}}_{p-\text{air}}(E/x_c)} \frac{d\sigma^{c\,(gg)}_{pp}(E/x_c, x_c)}{dx_c},$$

which allows to study the uncertainties at the level of c-quark production.

Ostapchenko, Garzelli, Sigl, Phys.Rev. D 107 (2023) 023014 [arXiv:2208.12185]

Sensitivity of $Z^c_{p-\mathrm{air}}(E)$ to scale variations

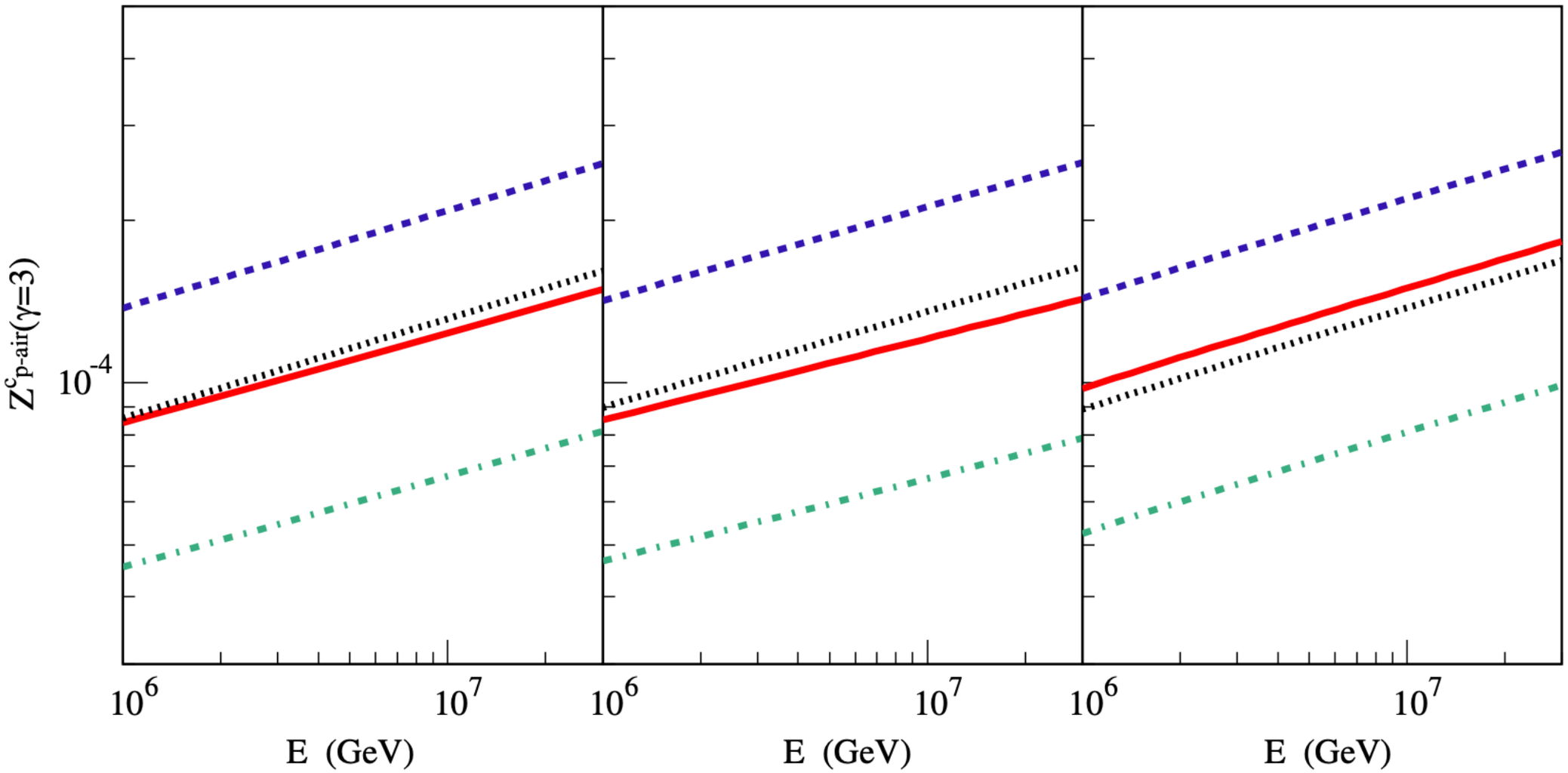

FIG. 6. CR spectrum-weighted moments of c-quark production spectrum $Z^c_{p\text{-air}}(E,\gamma)$, for $\gamma = 3$, calculated using different combinations of the factorization and renormalization scales: $(\mu_\mathrm{F},\mu_\mathrm{R}) = (1,1)m_{\perp_c}$ (solid), $(\mu_\mathrm{F},\mu_\mathrm{R}) = (2,1)m_{\perp_c}$ (dashed), $(\mu_\mathrm{F},\mu_\mathrm{R}) = (1,2)m_{\perp_c}$ (dot-dashed), and $(\mu_\mathrm{F},\mu_\mathrm{R}) = (2,2)m_{\perp_c}$ (dotted). The graphs in the left, middle, and right panels are based on gluon PDFs from ABMP16_3_nlo, CT14nlo_NF3, and NNPDF31_nlo_pch_as_0118_nf_3 PDF sets, respectively.

Ostapchenko, Garzelli, Sigl, Phys.Rev. D 107 (2023) 023014 [arXiv:2208.12185]

scale variation is the biggest uncertainty regarding the perturbative input for calculation of prompt neutrino fluxes

Summary of variations

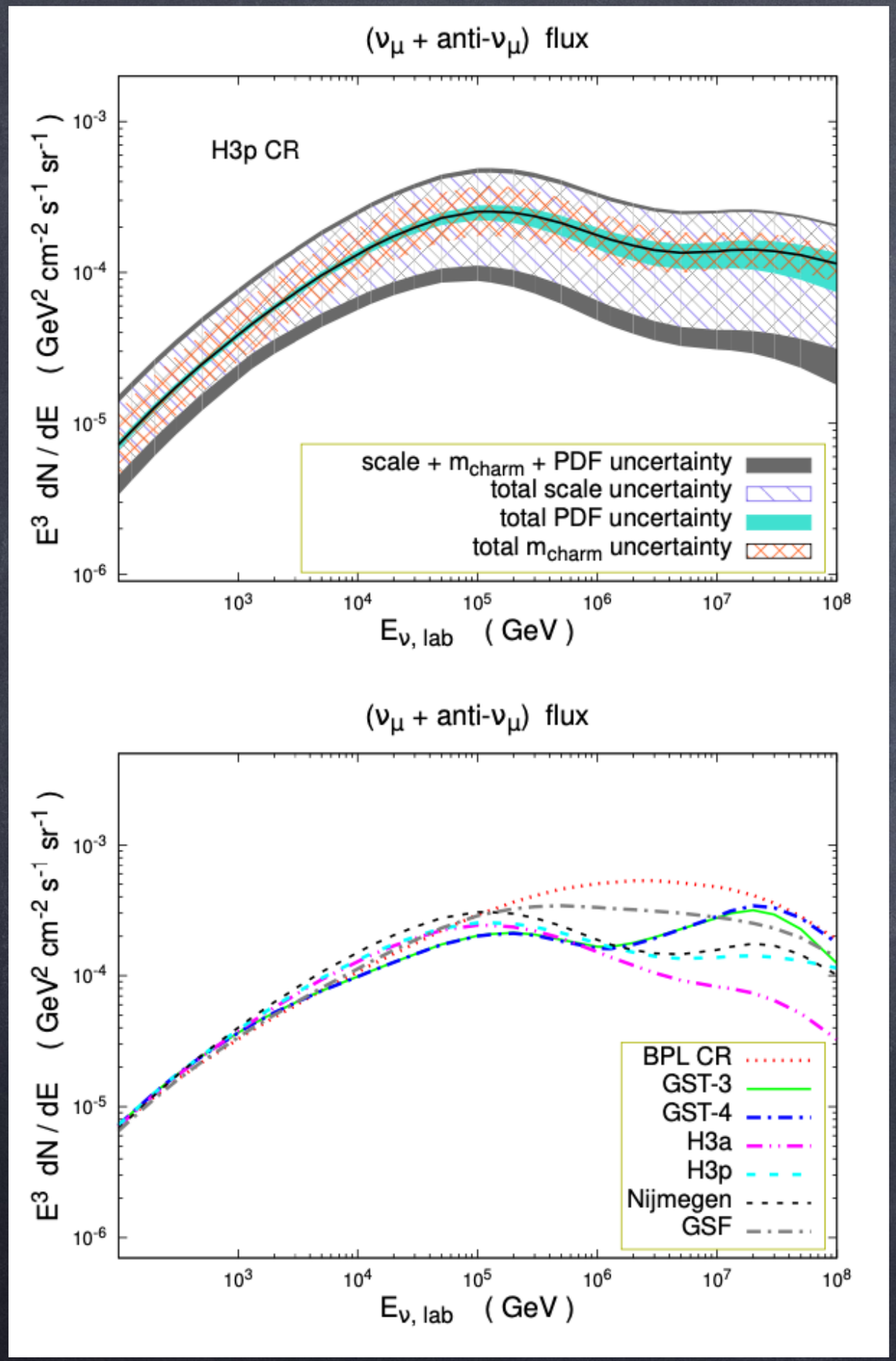

QCD uncertainties on prompt neutrino fluxes due to scale, PDF and charm mass variations, for a given cosmic ray all-nucleon flux.

Renormalization and factorisation scale uncertainties dominate

PDF uncertainties increase with neutrino energy due to sensitivity to smaller x at larger CM energies;

pole mass is ill-defined for confined particles

heavy hadrons are neglected here

uncertainties on prompt neutrino fluxes due to cosmic ray all-nucleon fluxes (mass composition)

O. Zenaiev et al., JHEP 04 (2020) 118 [arXiv:1911.13184] and Garzelli et al., proceedings ICRC 2021

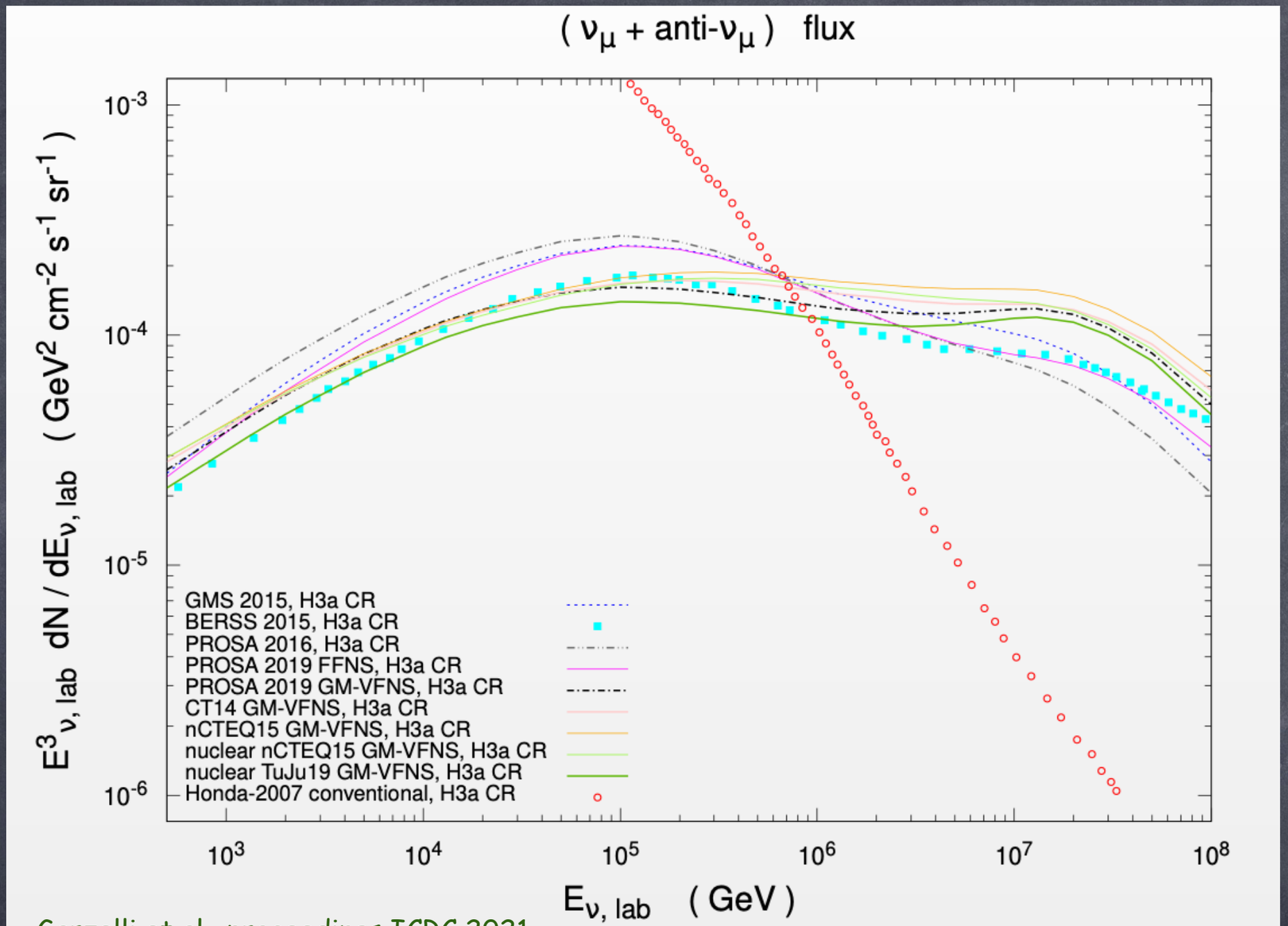

Garzelli et al., proceedings ICRC 2021

Figure 2: Central predictions for prompt (ν_μ + $\bar{\nu}_\mu$) fluxes using different approaches, adopting as input various proton and nuclear PDFs and charm mass values. Besides predictions shown here for the first time, we also present those of Ref. [3, 5, 10]. Predictions for conventional fluxes by Ref. [11], reweighted to the H3a CR primary all-nucleon spectrum, are also shown.

nuclear effects on prompt neutrino fluxes

approach 1: superposition model: use nucleon PDFs for A nucleons

approach 2: cold nuclear matter: uses nuclear PDFs

shadowing/anti-shadowing effects not large, roughly 10% effect for shadowing

differences are within scale uncertainties

pA runs at LHC, new experiments sensitive to forward neutrinos (SND@LHC) and data from electron-ion collider (EIC) and large hadron-electron colliders (LHeC) will further constrain nuclear PDFs

nuclear effects on prompt neutrino fluxes

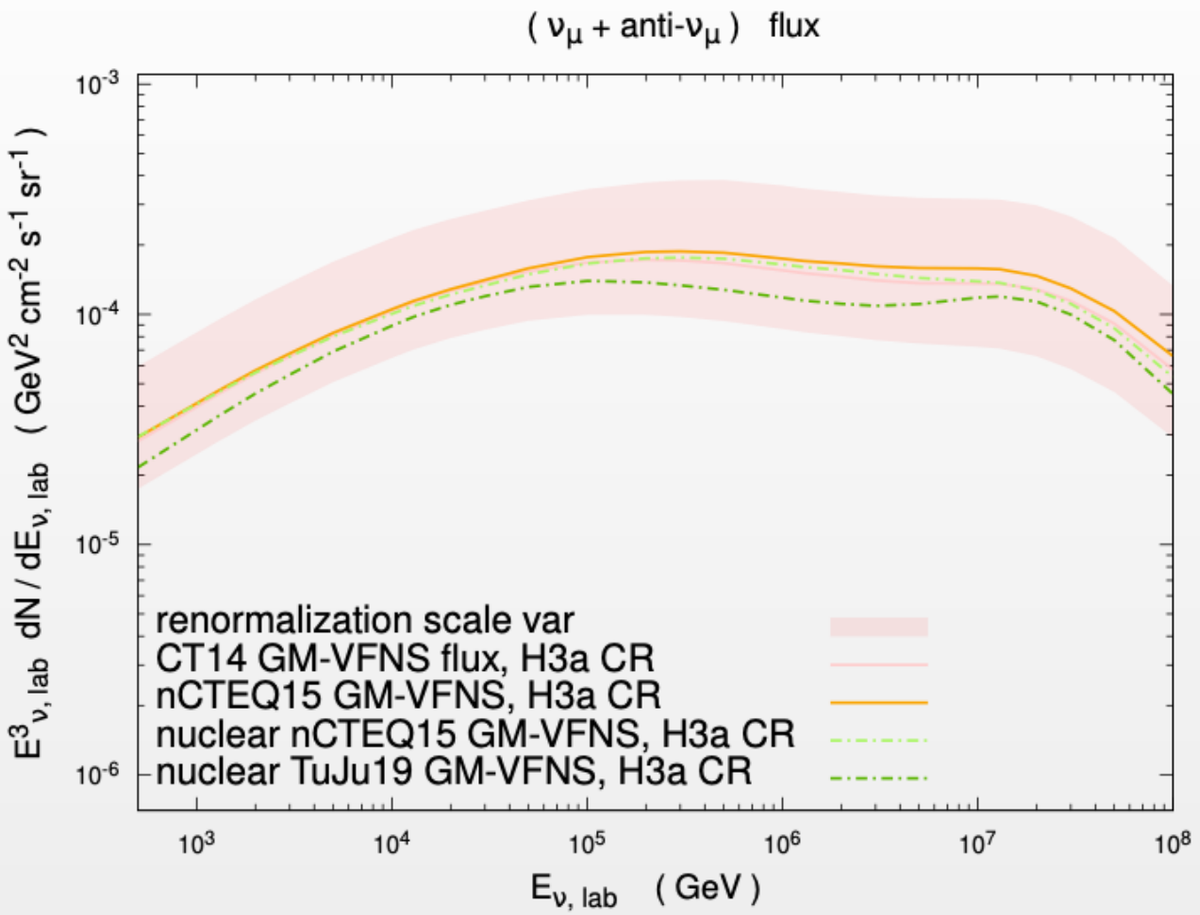

* Predictions using nuclear PDFs within scale uncertainty bands of those with proton PDFs and superposition model.

* Suppression of prompt fluxes due to CNM effects ?
only moderate shadowing for low-mass nuclei....
$\Rightarrow$ to be better tested at future colliders.

the largest contribution to the prompt $\nu_\mu + \bar{\nu}_\mu$ flux comes from the charmed mesons $D^0 + \bar{D}^0$ and $D^+ + D^-$

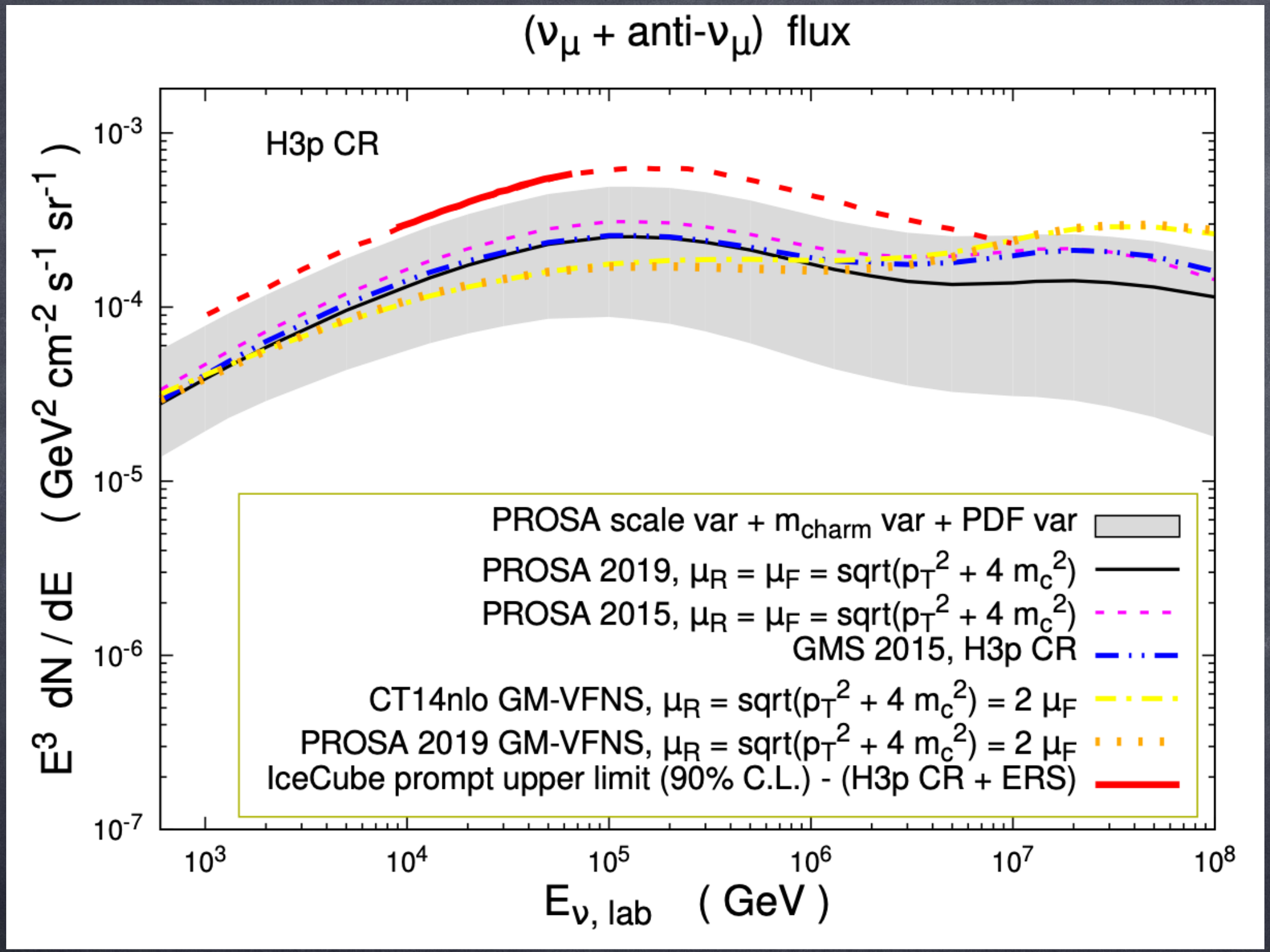

comparison to other predictions

note: slope differences are due to different factorisation scales

O. Zenaiev et al., JHEP 04 (2020) 118 [arXiv:1911.13184]

Introduction to intrinsic charm

proton Fock states $|uud\bar{c}c\rangle$ and $|uud\bar{c}c\bar{c}c\rangle$: momentum fraction carried by c should be significant ~ 0.3 due to comparable velocities.

Gluon/photon exchange gives rise to $pp \to \overline{D^0} + \Lambda_c^+ + X, \bar{D}^{0*} + \Lambda_c^+ + X, \cdots$, upon interaction with another proton or a lepton (deep inelastic scattering)

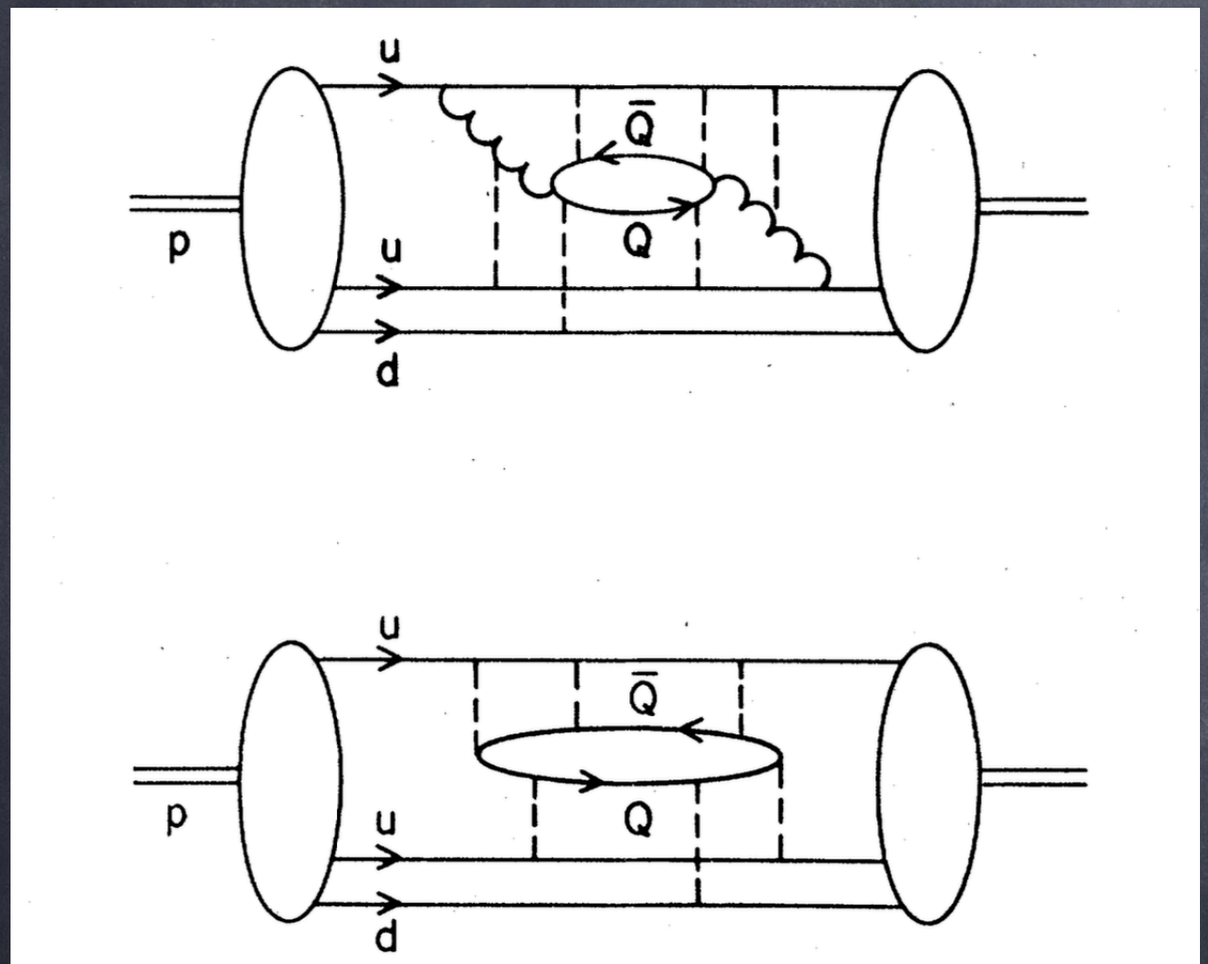

FIG. 1. Diagrams which give rise to the intrinsic heavy quarks ($Q\bar{Q}$) within the proton. Curly and dashed lines represent transverse and longitudinal-scalar (instantaneous) gluons, respectively.

Brodsky et al., Phys. Rev. D 23 (1981) 2745, Phys.Lett. 93B (1980) 451

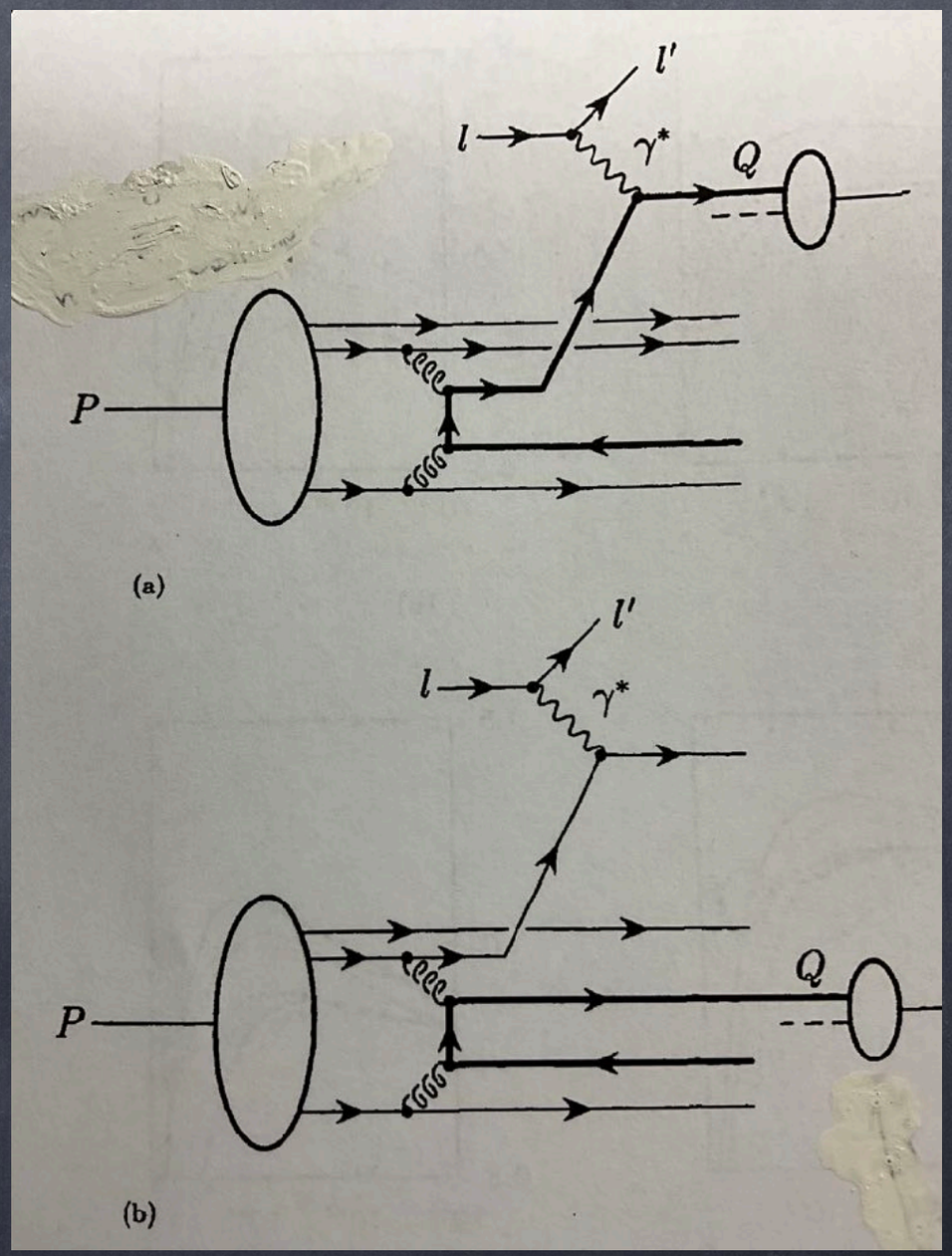

Graudenz., Fortschr. Phys. 45 (1997) 629

Old Evidence for Intrinsic Charm ?

Performances of the PROSA QCD computation of *D*-meson production w.r.t. LEBC-EHS exp. data

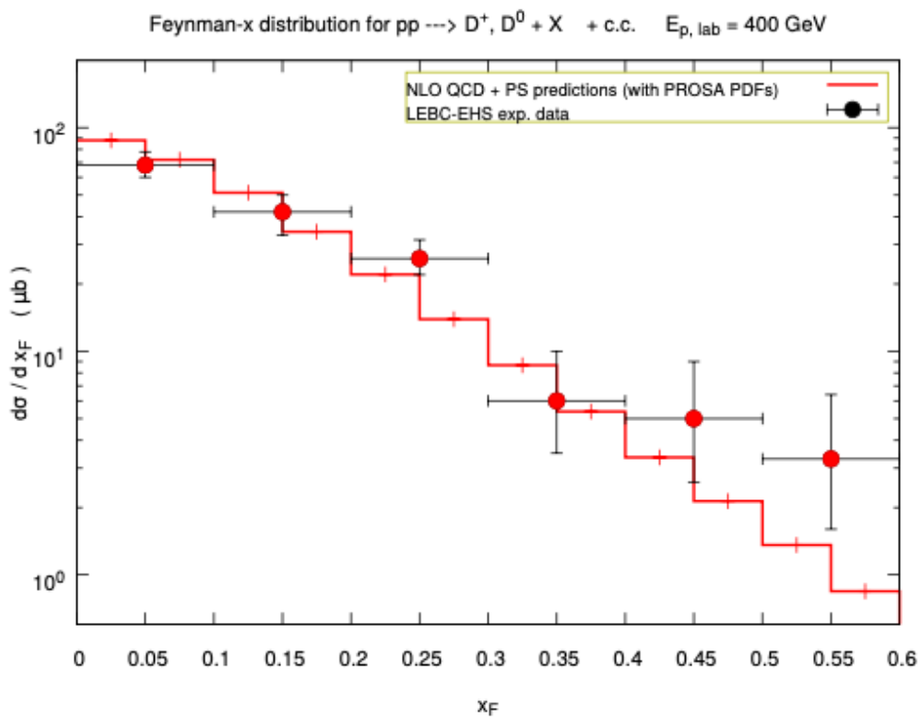

PROSA

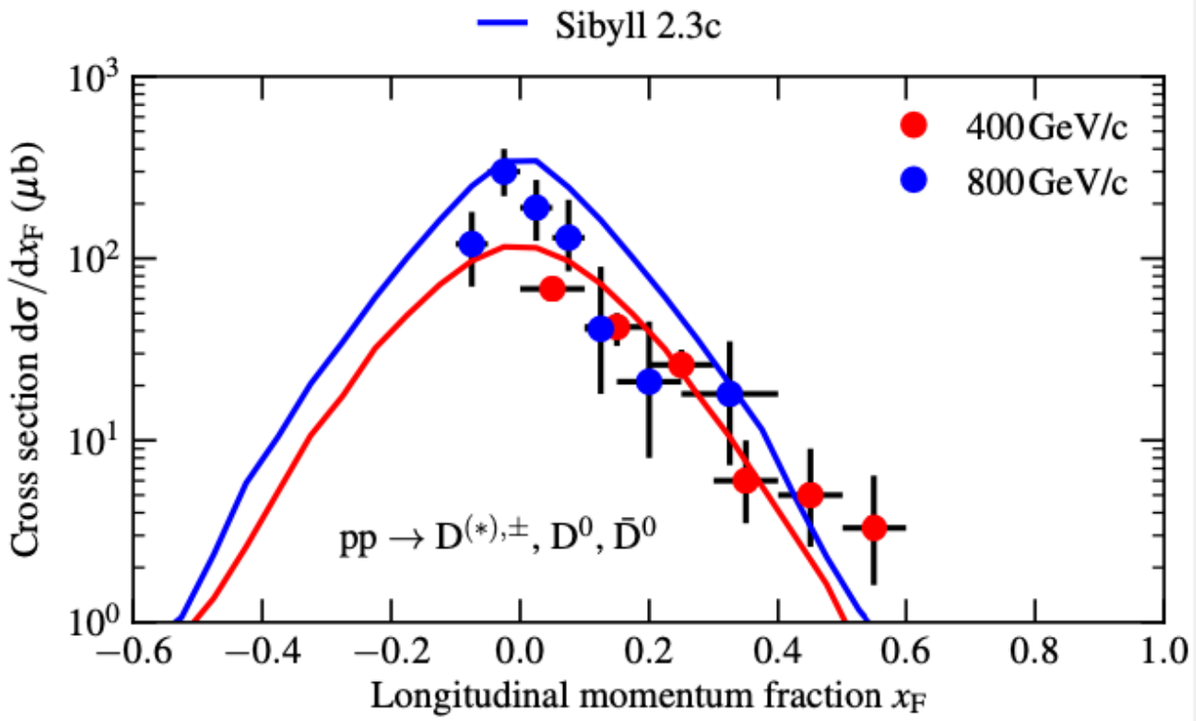

SIBYLL

* Fixed target experiment with $E_{p,\,lab} = 400$ GeV.
* Measure relatively large $x_F = p_{z,D}/p_{z,D}^{max}$ (up to $x_F \sim 0.6$).
* Sizable QCD uncertainty band not included in the plot.

Old Evidence for Intrinsic Charm ?

Performances of the PROSA and SIBYLL computation of *D*-meson production w.r.t. LEBC-MPS exp. data

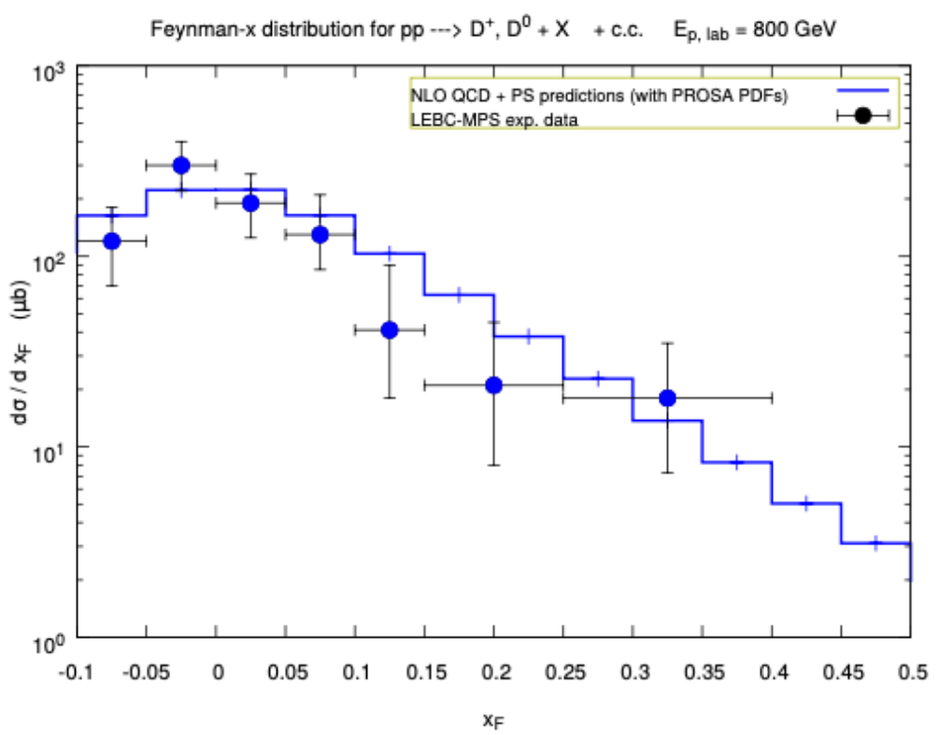

PROSA

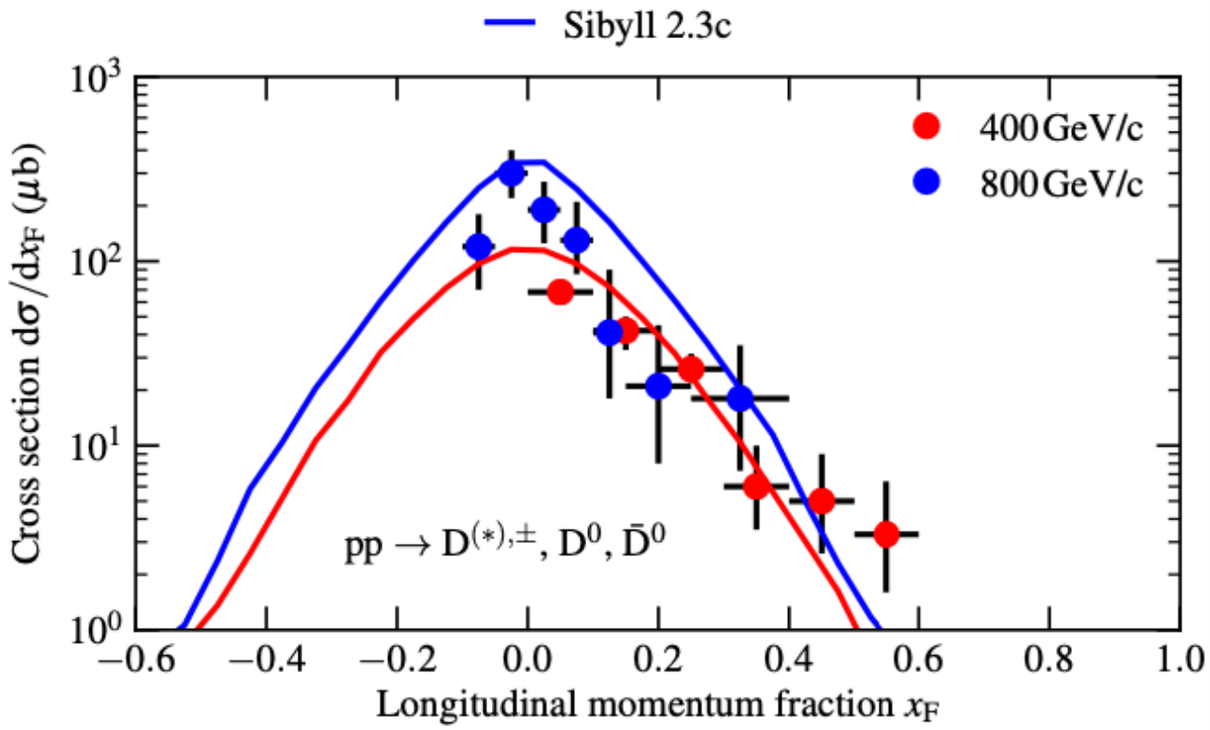

SIBYLL

* Fixed target experiment with $E_{lab} = 800$ GeV.
* Measure relatively large x_F (up to $x_F \sim 0.4$).
* Sizable theory QCD uncertainty band not included in the plot.

Evidence for intrinsic charm ?

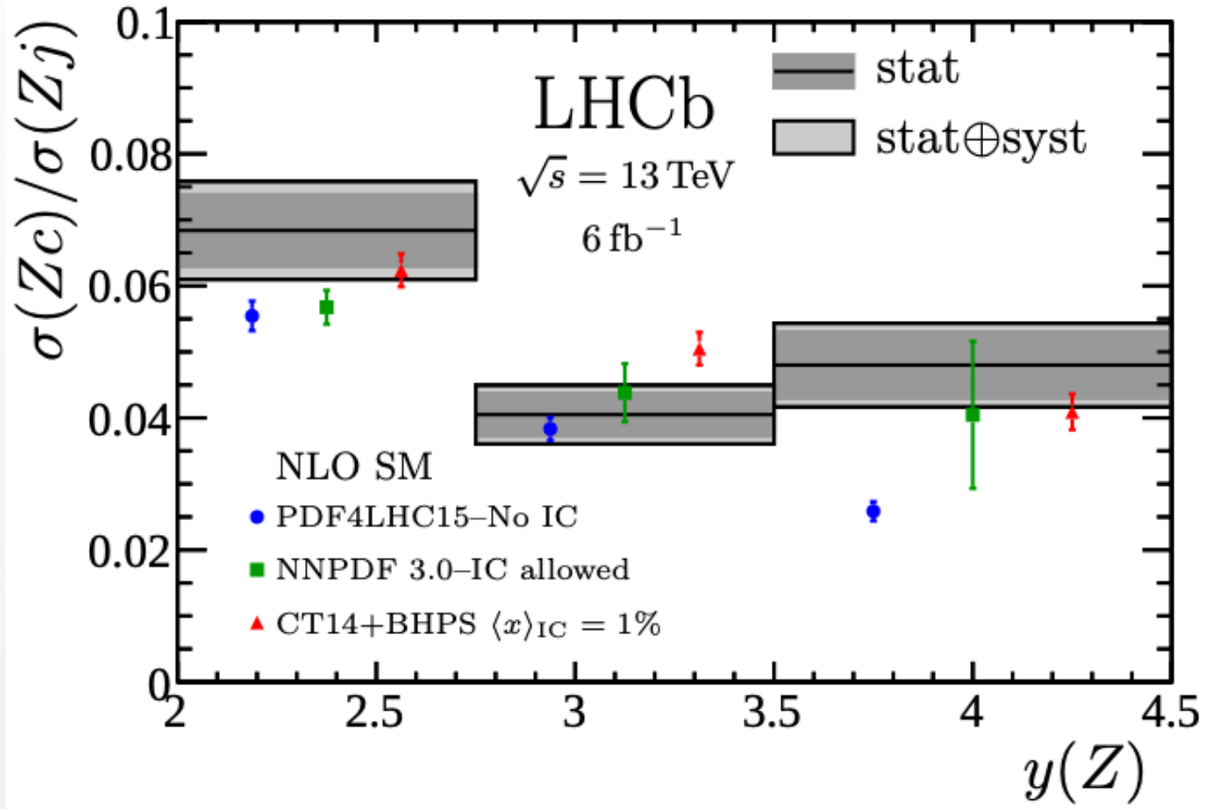

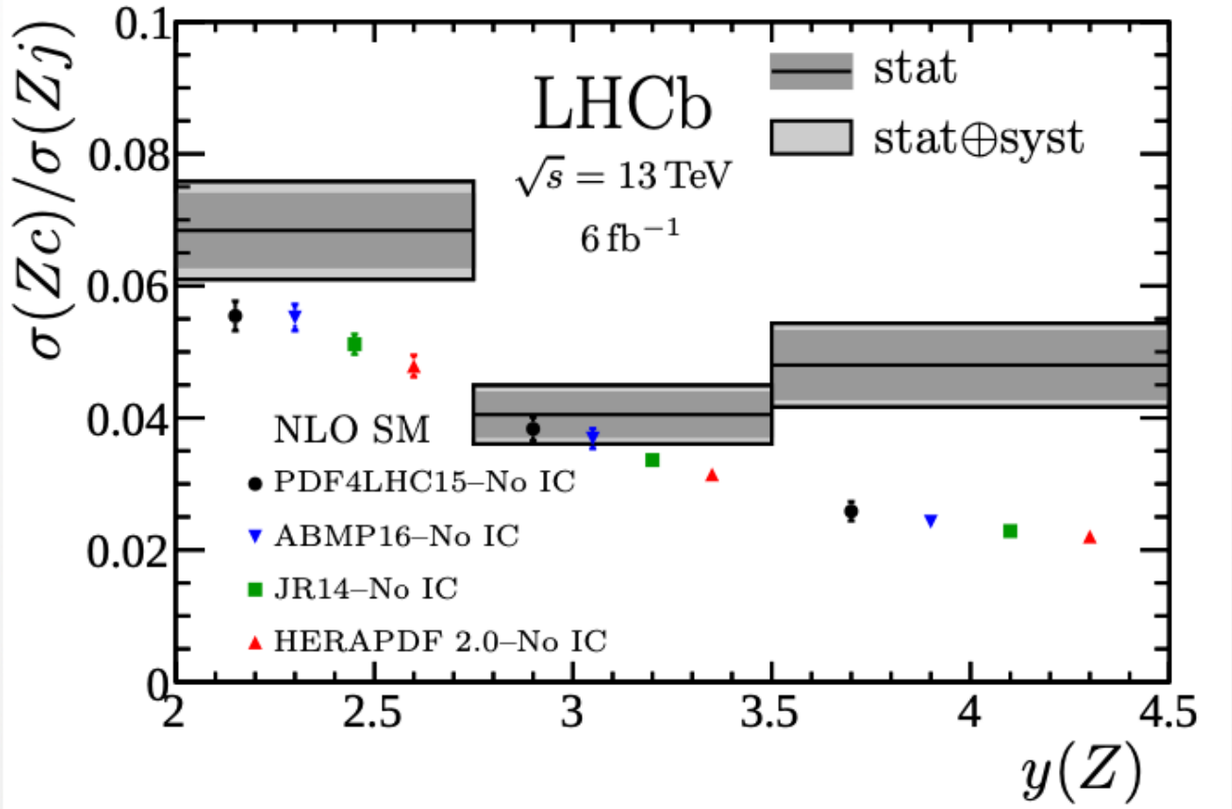

LHCb collaboration, Phys.Rev.Lett. 128 (2022) 082001

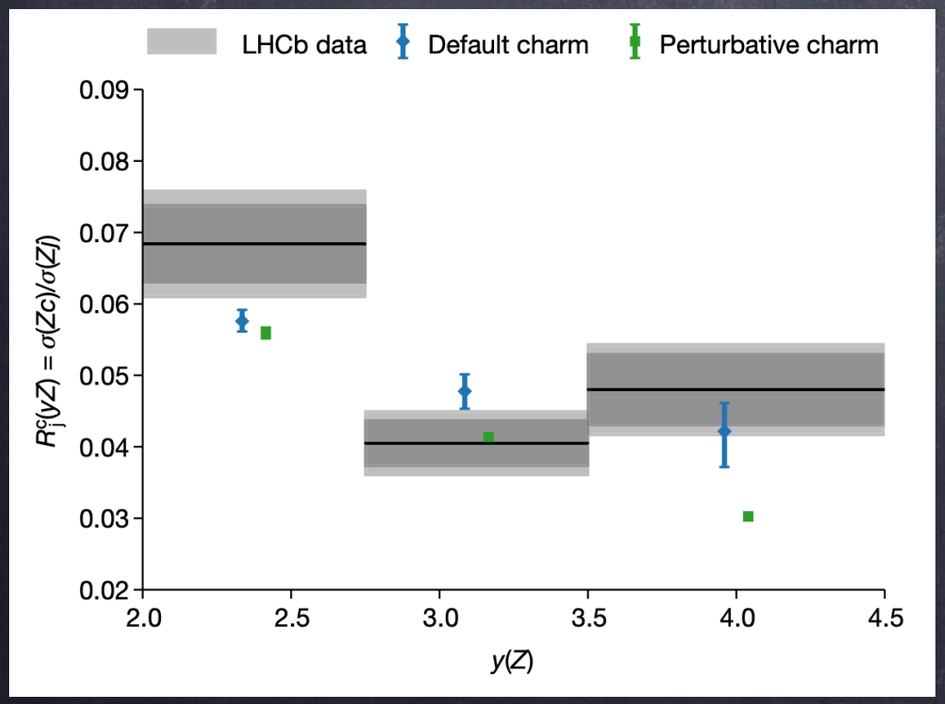

Fraction of charmed jets in 3 rapidity intervals

NNPDF collaboration, Nature 608 (2022) 483

Differential Cross Section for intrinsic charm production

$$\frac{d\sigma^{c(\mathrm{intr})}_{p-\mathrm{air}}(E,x_c)}{dx_c} = w^c_{\mathrm{intr}}\,\sigma^{\mathrm{inel}}_{p-\mathrm{air}}(E)\,f_c^{(\mathrm{intr})}(x_c)\,,$$

with w^c_{intr} the overall weight of proton Fock states containing IC contributing to the inelastic cross section and $f_c^{(\mathrm{intr})}(x)$ the constituent c-quark light-cone momentum fraction distribution, normalised to unity:

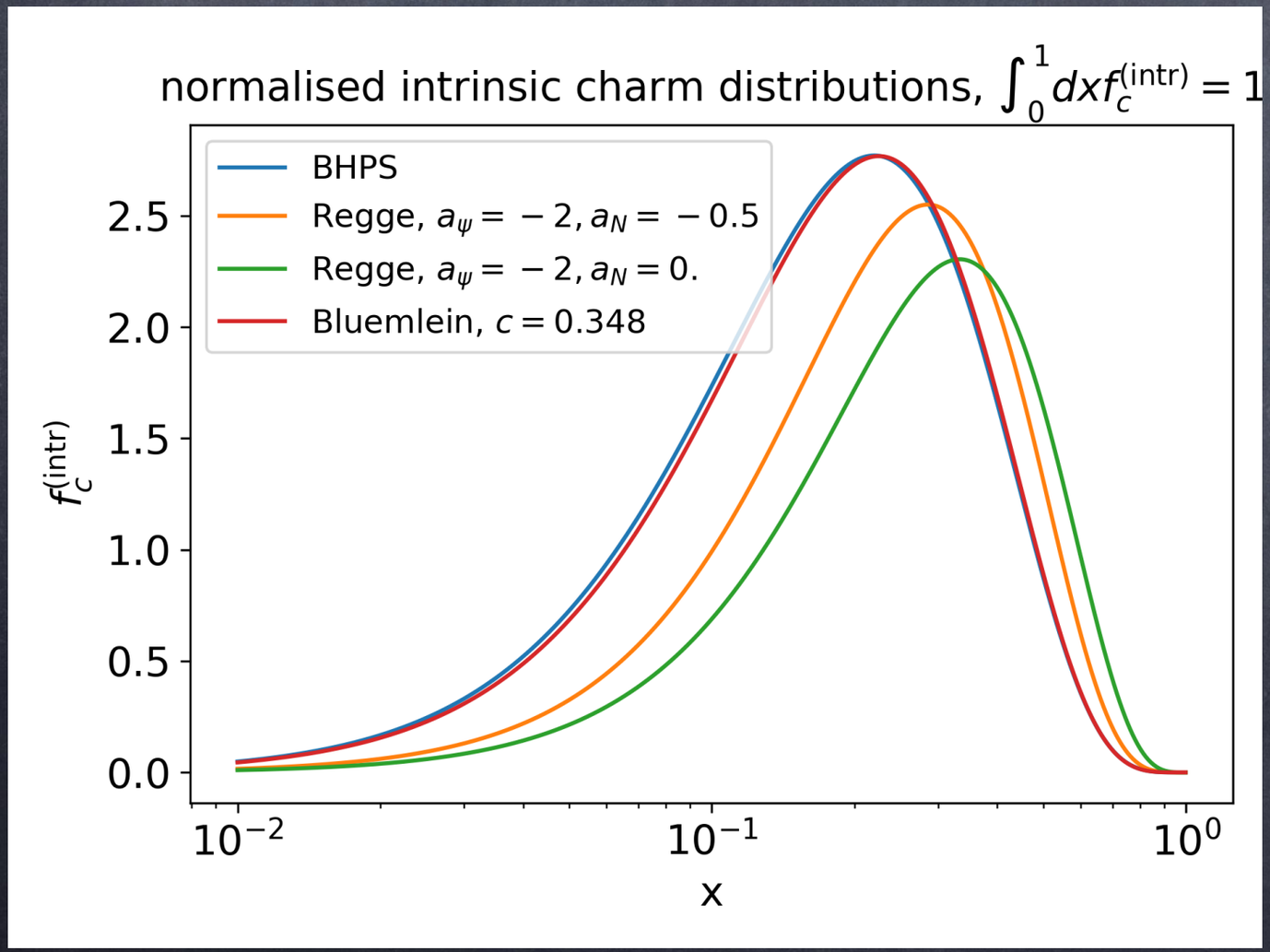

Functional shape motivated by the valence quark distribution on slide 11.

For example, in the Meson Baryon Model based on Hobbs, Londegan, Melnitchouk, PRD 89 (2014) 074008 one obtains

$d\sigma/dx$ distribution in Melnitchouk model

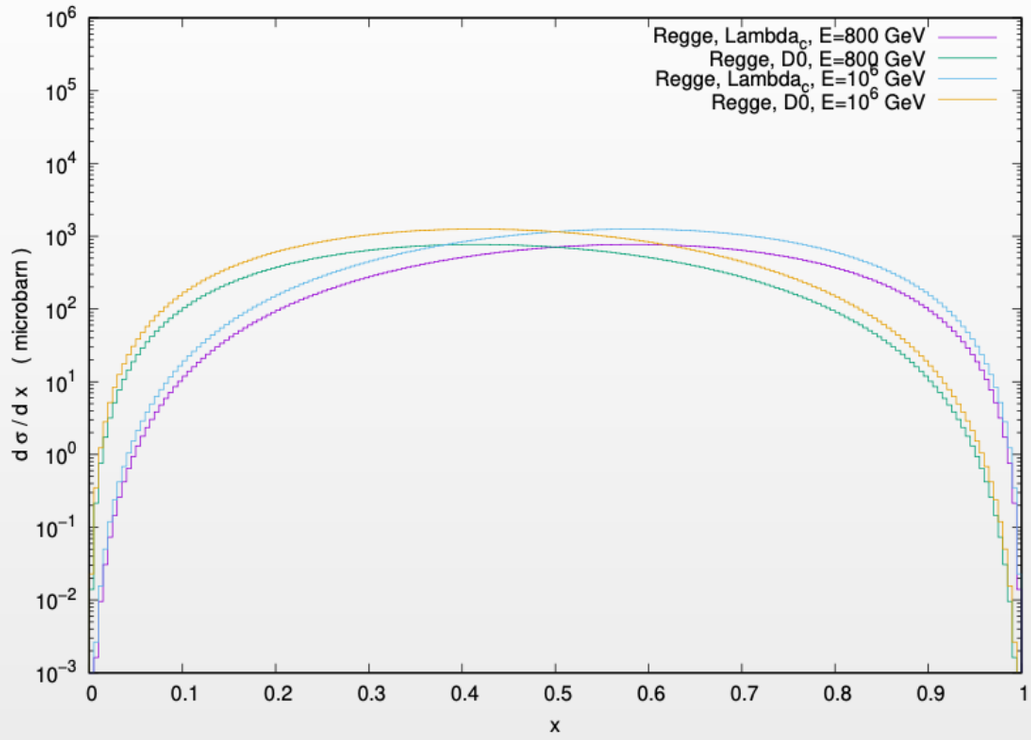

* Comparison of $d\sigma/dx$ distributions for collisions at $E_{proj,lab} = 800$ GeV and $E_{proj,lab} = 10^6$ GeV. for $w_{IC} = 0.01$

Main ingredient for the calculation of the $Z_{p-\mathrm{air}}^{D^0(\mathrm{intr})}$ and $Z_{p-\mathrm{air}}^{\Lambda_c(\mathrm{intr})}$ which enter the cascade equations for the prompt fluxes.

For IC one can approximate the Z-moment as

$$Z_{p-\mathrm{air}}^{c(\mathrm{intr})}(\gamma_p) = Z_{pp}^{c(\mathrm{intr})}(\gamma_p) = w_{\mathrm{intr}}^{c} \int dx_c \, x_c^{\gamma_p - 1} \, f_c^{(\mathrm{intr})}(x_c) \,,$$

This is neither energy nor target dependent, causing a neutrino flux which follows the primary CR spectrum. In contrast, the prompt component from perturbative charm production is flatter than the primary spectrum.

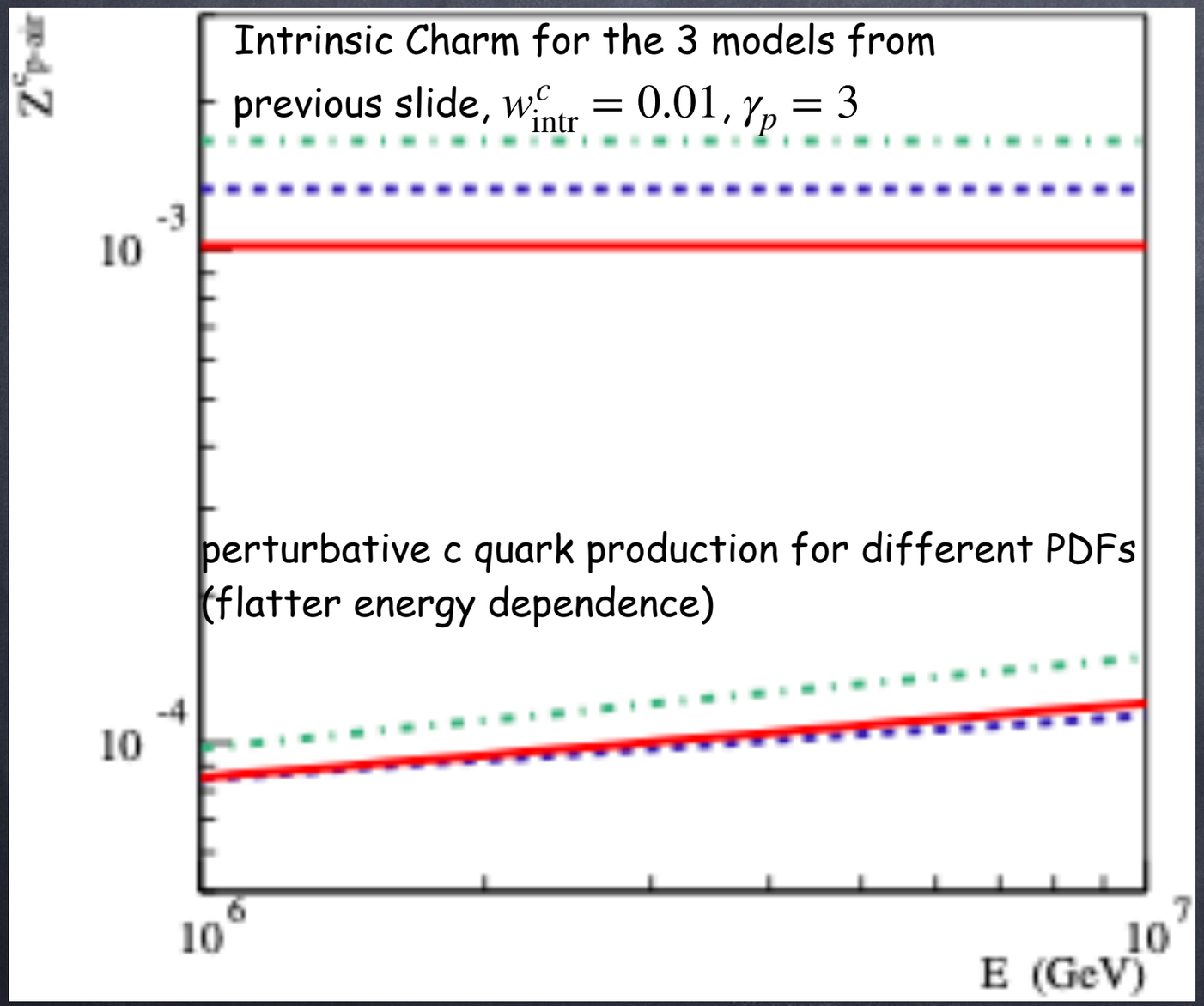

note that the normalisation of IC moments is quite uncertain due to different hadronisation of constituent quarks

IceCube limits on IC in Melnitchouk model

In IC Melnitchouk model there are two contributions to $\bar{D}^0$: prompt $\bar{D}^0$ and $\bar{D}^0$ from $\bar{D}^{*0}(2007)$ decay.

central IC and pQCD

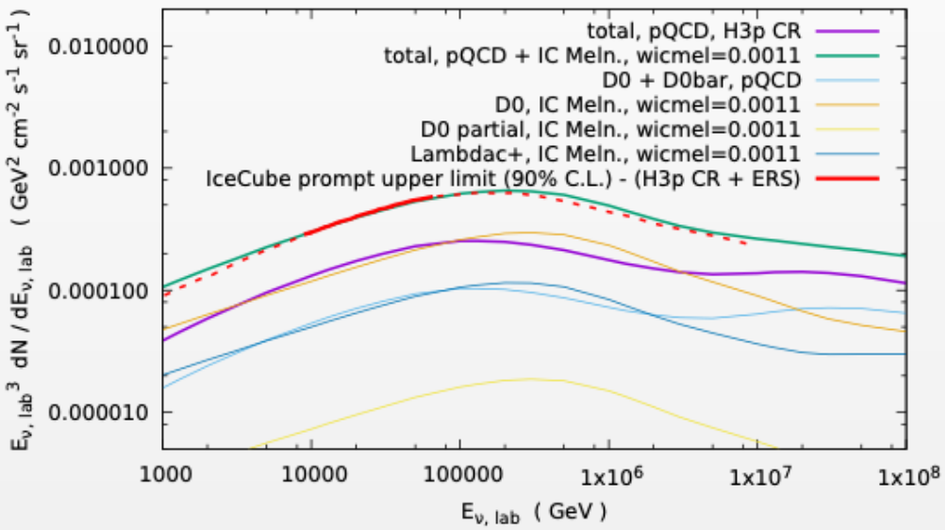

preliminary

minimum IC, maximum pQCD

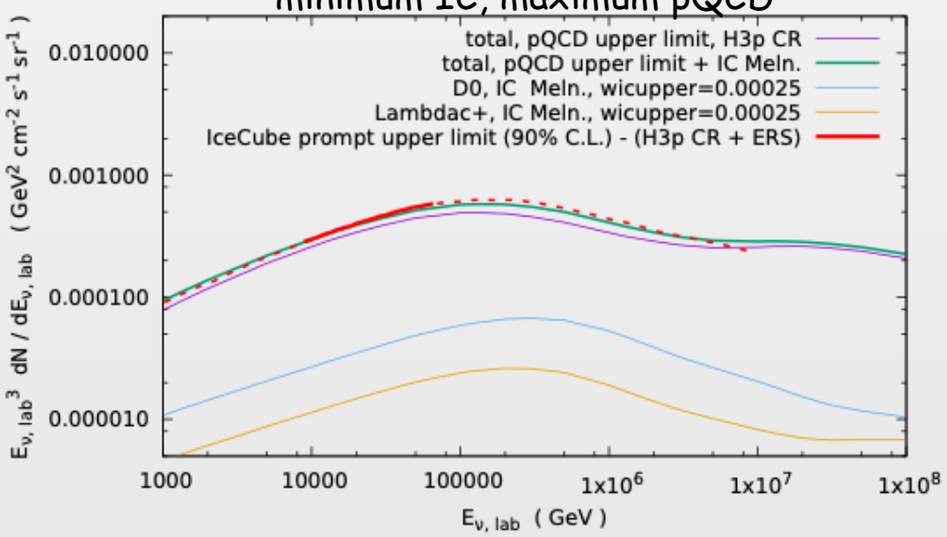

maximum IC, minimum pQCD

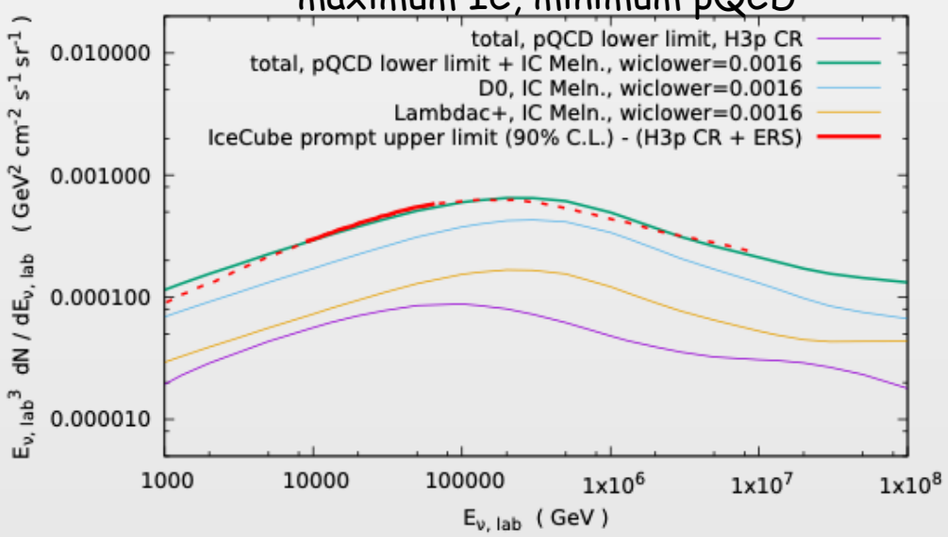

w_{IC} constrained in the interval [0.00025, 0.0015], with central value 0.0011.

with $w_{IC} = w_{IC}^{(0)} w_{IC}^{c(\mathrm{frag})}$ where $w_{IC}^{(0)}$ is the IC content of the proton and $w_{IC}^{c(\mathrm{frag})}$ is the probability to "free" intrinsic charm quarks from their virtual state and hadronize them.

Garzelli, Ostapchenko, Sigl, to appear

IceCube limits on IC in Regge model ($\alpha_n = -0.5$)

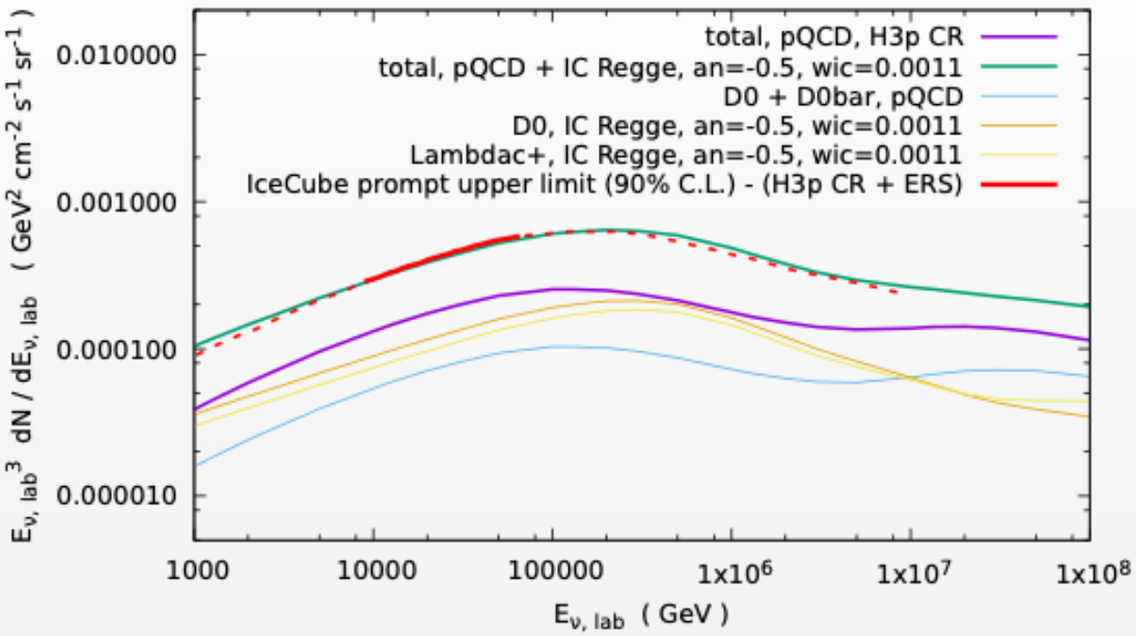

preliminary

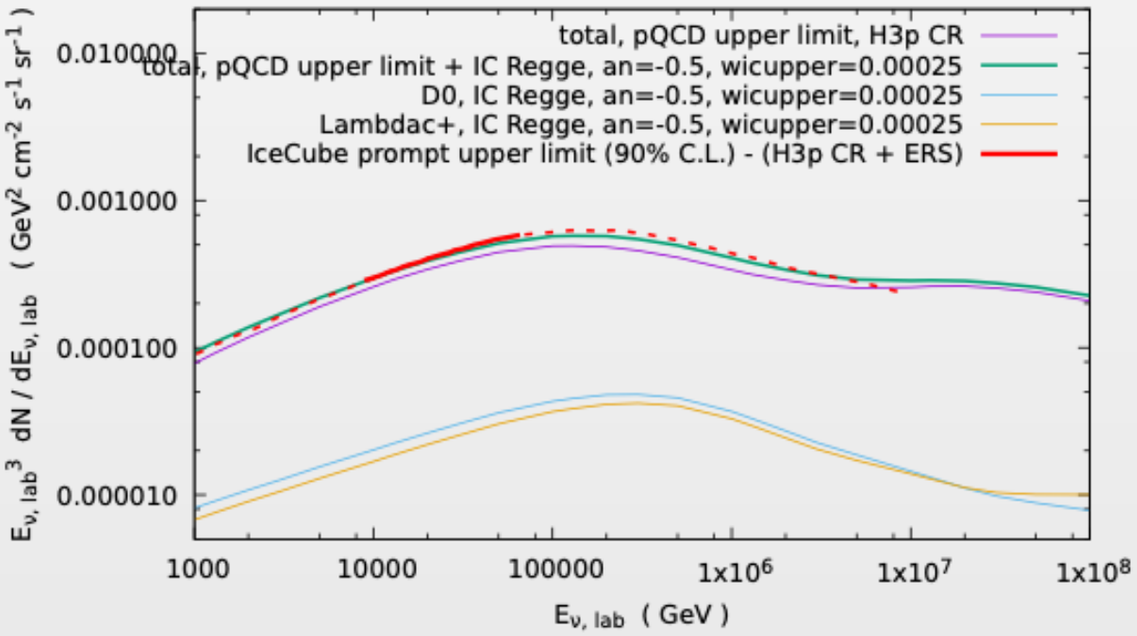

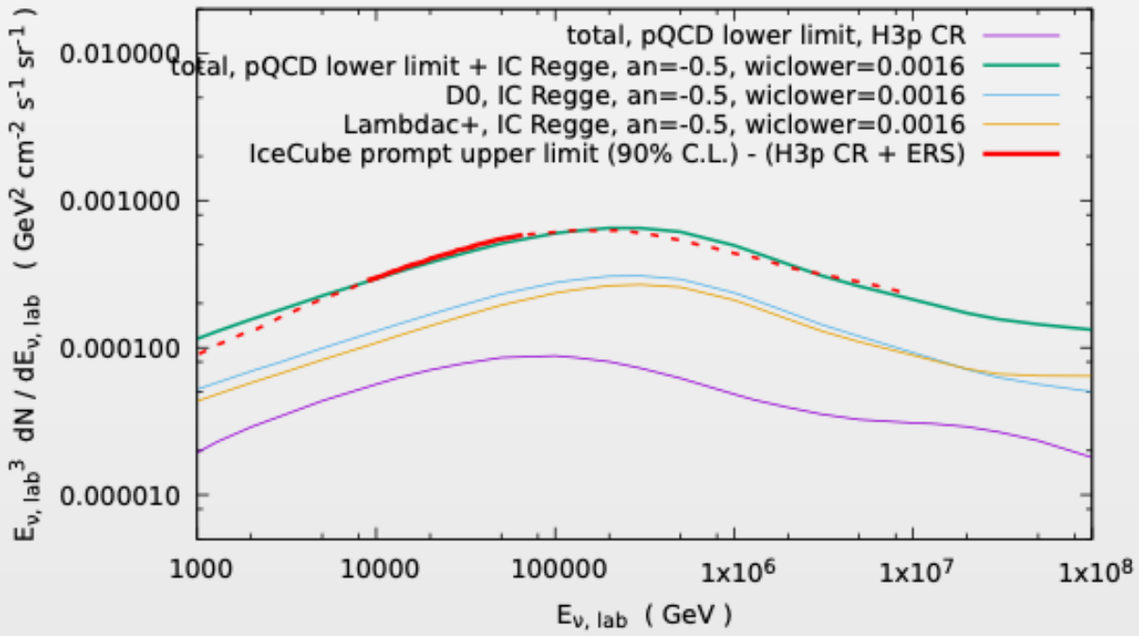

w_{IC} constrained in the interval [0.00025, 0.0016], with central value 0.0011.

IceCube limits on IC in Regge model ($\alpha_n = 0$)

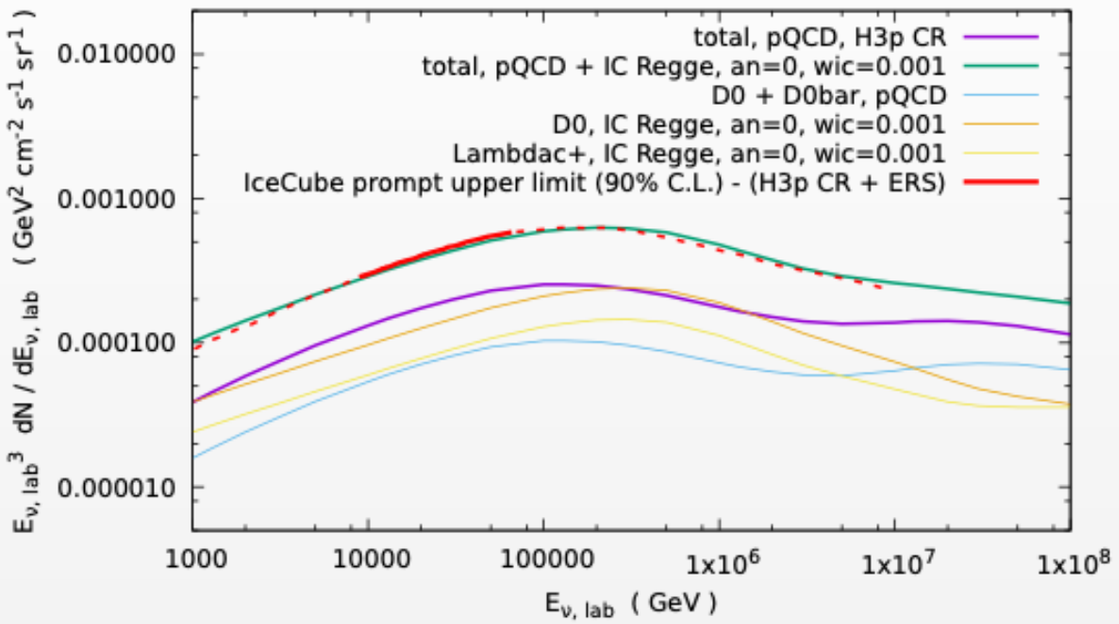

preliminary

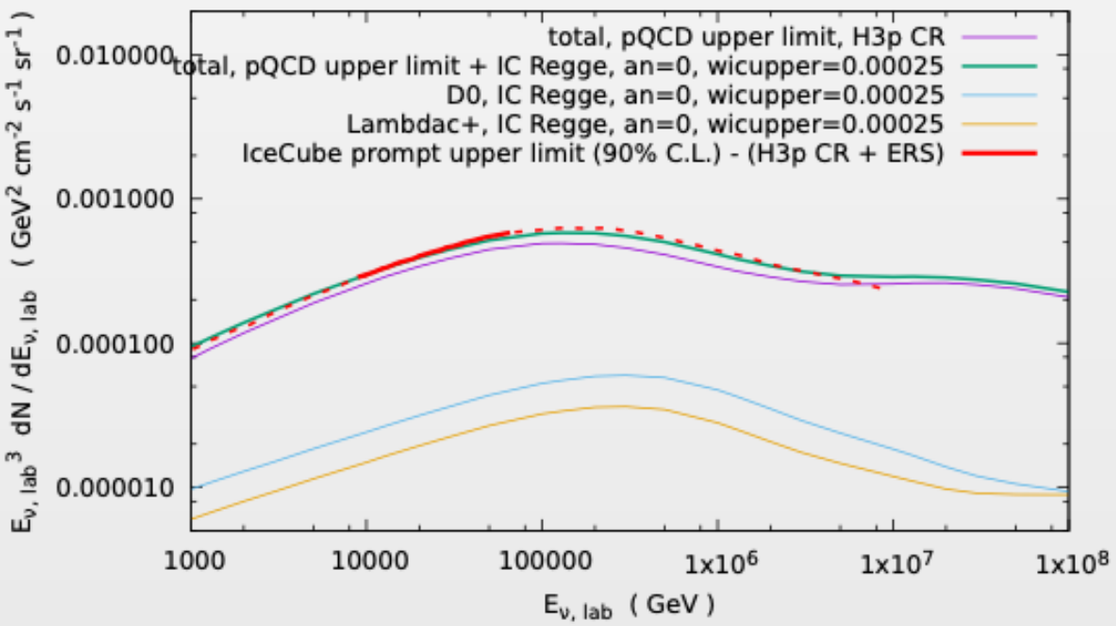

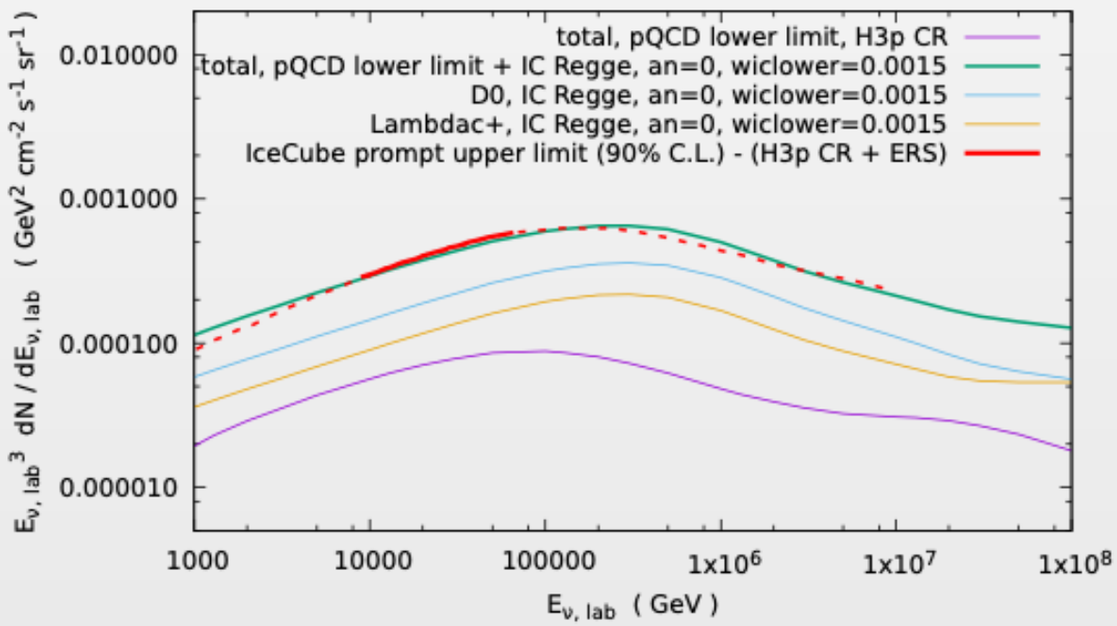

w_{IC} constrained in the interval [0.00025, 0.0015], with central value 0.0010.

Charm component in modern PDFs (CT14)

$\mu_F = 2.5$ GeV

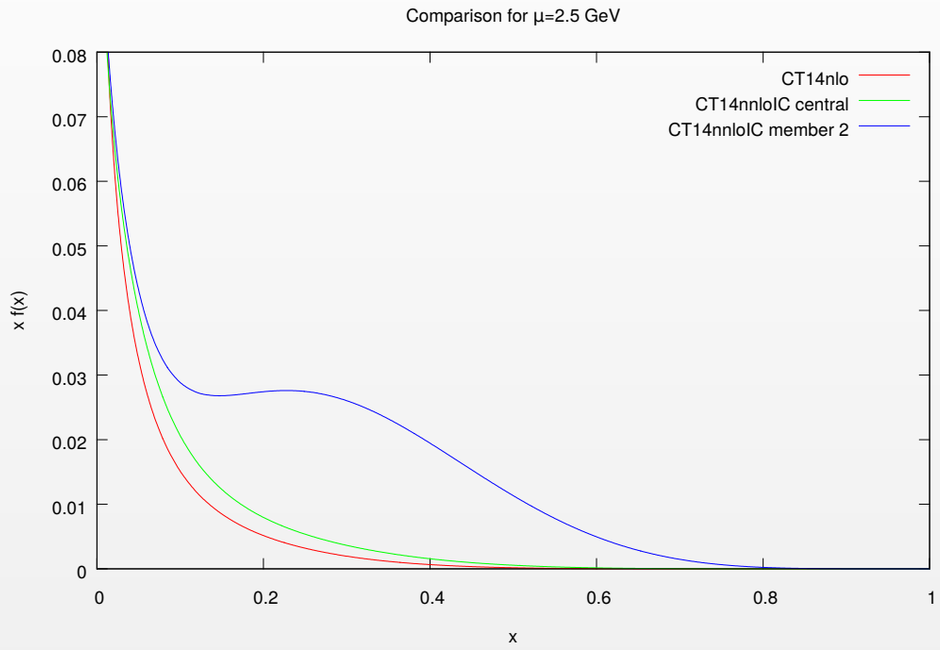

$\mu_F = 10$ GeV

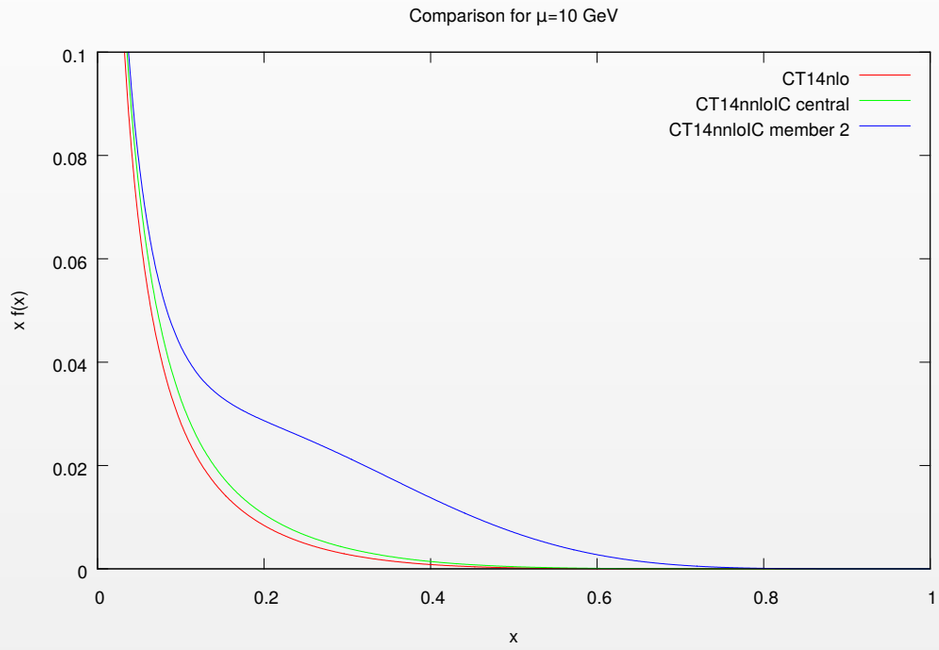

lin

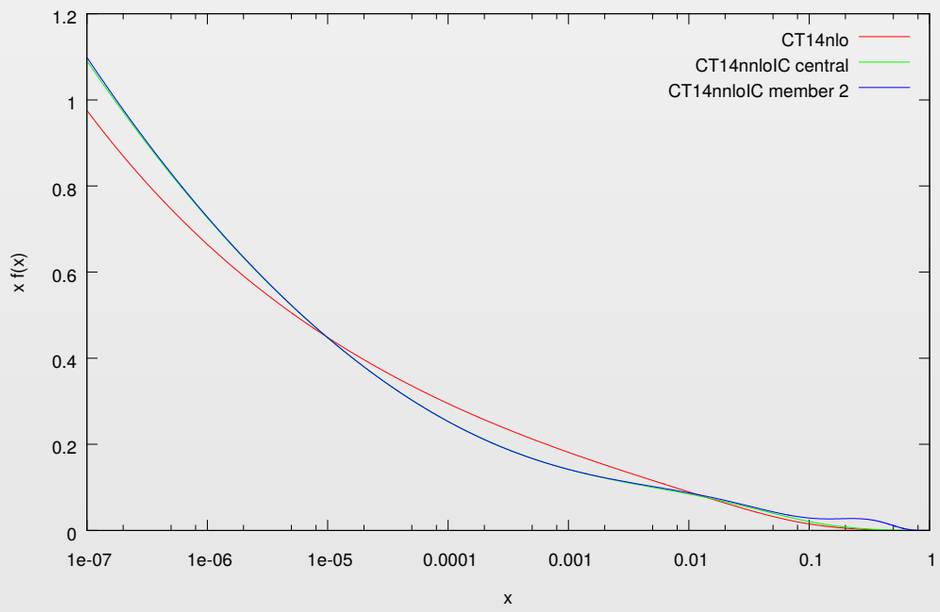

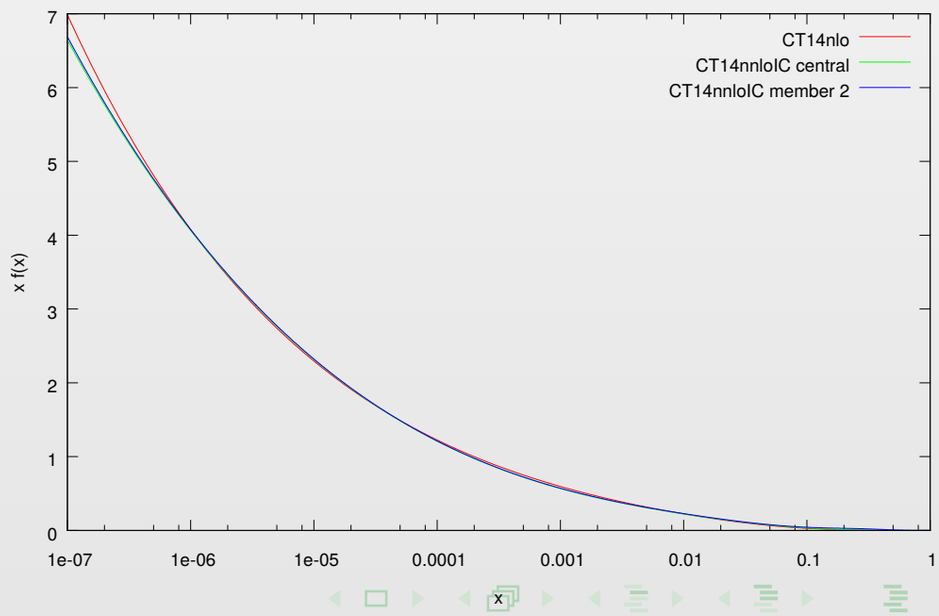

log

lower lines are standard PDF sea quarks, blue is intrinsic charm PDF (sea plus valence)

Prompt Neutrino Fluxes with intrinsic charm PDFs

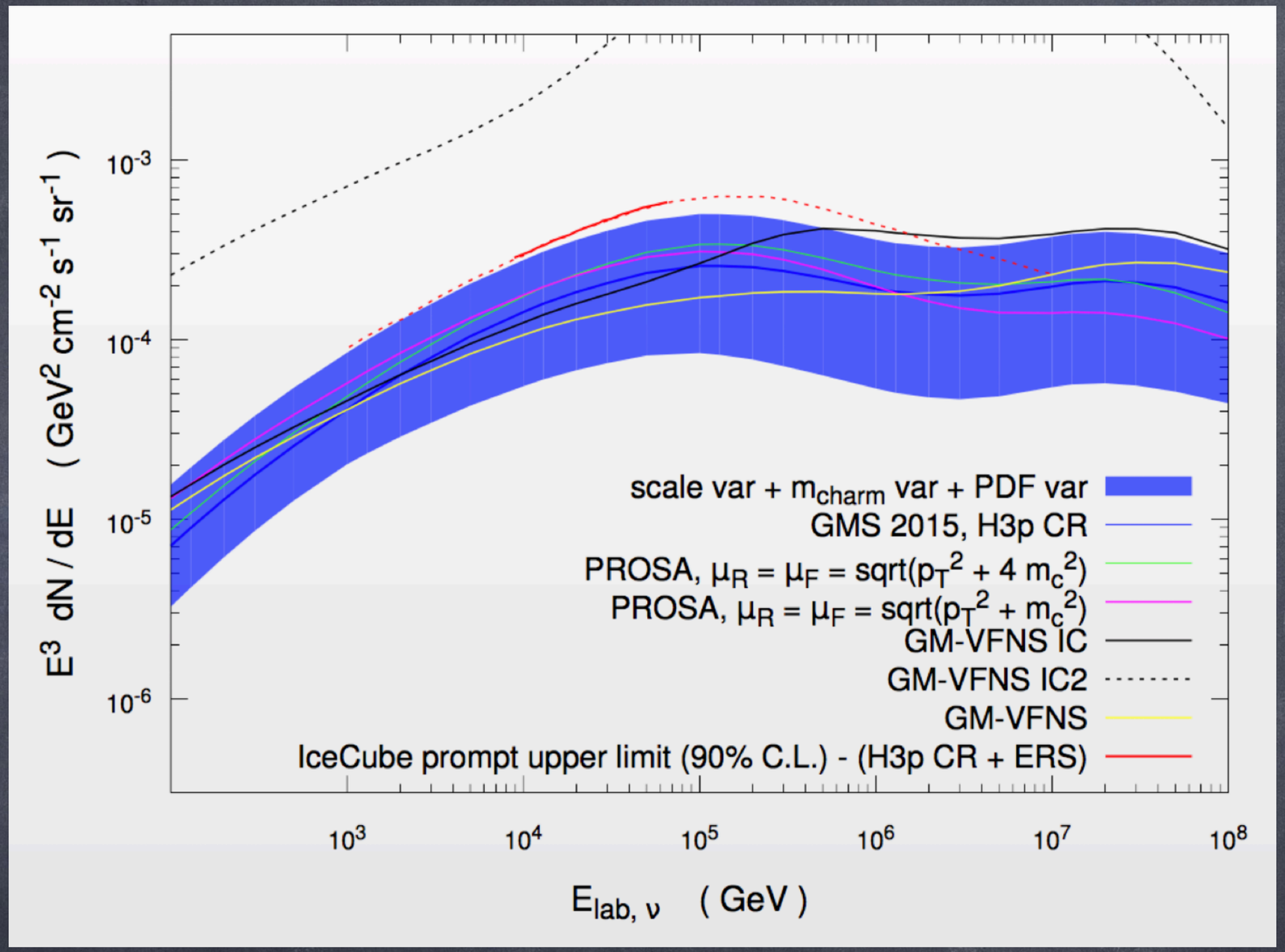

here it is assumed that hadronization of intrinsic charm and perturbative charm is identical; intrinsic charm is contained only in the PDF

Other calculations:

Halzen and Wille, Phys. Rev. D 94 (2016) 014014 [arXiv:1605.01409] (upper limits compatible with our results)

Laha and Brodsky, Phys. Rev. D 96 (2017) 123002 [arXiv:1607.08240 claims smaller upper limits]

Conclusions

1.) Recent updates on prompt neutrino component based on latest QCD results and data, in particular LHCb, are important to interpret HE neutrino fluxes and disentangle astrophysical from atmospheric neutrinos.

2.) Deduced uncertainties are relatively large, up to a factor ~ 5; dominated by QCD and above ~ 10^6 GeV by poorly understood cosmic ray all-nucleon flux

3.) Below the "knee" atmospheric prompt neutrinos from intrinsic charm have slightly softer spectrum than prompt neutrinos from perturbative charm production and can thus potentially be disentangled. This allows to put constraints on IC from IceCube data.

4.) Limit on contribution of intrinsic charm to the total prompt neutrino flux is of order 0.001 (including fragmentation effects), rather independently of the intrinsic charm model

Backup Slides

Uncertainties in the heavy-quark content of PDFs

* Ansatz:
  charm and bottom in the nucleon PDFs are radiatively generated:
  - for scales $\mu_F \leq m_c$ ($\mu_F < m_b$) no charm (bottom) in PDFs
  - for scales $\mu_F > m_c$ ($\mu_F > m_b$) charm (bottom) is produced by QCD evolution through $g \to c\bar{c}$ and $c \to gc$ splittings ($g \to b\bar{b}$ and $b \to gb$ splittings)

* Further possibility:
  additional non-perturbative charm and bottom components:
  $\Rightarrow$ Models for intrinsic charm/bottom.

  Original motivation: old experimental data at large x_F.
  But, no need for intrinsic charm/bottom at LHC
  (at least for the observables studied so far).
  Possible probe of the (non-)existence of intrinsic charm at LHC:
  $pp \to Zc, \gamma c$